POLITECNICO DI MILANO

School of Industrial and Information Engineering

Energy Department – Piacenza Campus

NTNU

NORWEGIAN UNIVERSITY OF SCIENCE AND TECHNOLOGY

Faculty of Engineering Science and Technology

Department of energy and Process Engineering

MASTER OF SCIENCE IN ENERGY ENGINEERING FOR AN ENVIRONMENTALLY SUSTAINABLE WORLD

Development and test of a reaction system for direct liquefaction of Biomass in Hydrothermal Media

Advisor: PhD Candidate Quang Vu Bach

Supervisors: Dr. Khanh-Quang Tran

Dr. Federico Vigano

Thesis Dissertation of:

Jesus David Hernandez Ortiz.

Academic Year 2013-2014

This work, and my whole academic career,

is dedicated to God, the father almighty, and to my parents,

to whom, I owe absolutely everything.

Acknowledgments

My most sincere thanks to Profesor Khan-Quan Tran, for having giving me the opportunity of working with him in this new system, and for having opened the doors of the NTNU Thermal lab to me. So far, these last months of hard work in the thermal lab have been really instructive, as no other lesson in my academic life.

To my friend Quang Vu Bach, for his support and help in all the practical issues in the lab. Not to mention for the invitations to the pizza gatherings!

To Reidar, Halvor and Helge in the Thermal Lab, for having been so helpful throughout the whole development process if the system.

To my tutor at Politecnico di Milano, Professor Federico Vigano, for having supported this project since the very beginning. Without his support, this great experience in Norway would not have been possible.

To my friends: Felix, Camila and especially to Joana, for having shared with me the coldest and longest nights of my life. You were my <u>survival box</u> of happiness in the far north.

Table of Contents

List of Figures

List of Tables

Abstract

Hydrothermal liquefaction is a promising technology for converting plant biomass directly to liquid fuels with better fuel properties compared to traditional fast pyrolsyis. The technology employs water, in subcritical conditions as reaction media, and therefore is very suitable for wet biomass feedstock including agricultural waste. It can also be employed to pre-treat plant biomass for bio-ethanol production. However, the conversion efficiency and selectivity of the techology need to be improved. One way to meet the needs is to apply the concept of process intensification with regards to reactor design. By miniturization of the reactor size, apart from other benefits, heat and mass transfer within the reactor can significantly be improved, which in turn help improve the conversion efficiency and selectivity of the process.

In this project, a semi continuous flow fixed bed reactor system was designed and developed. In addition, the system was used to experimentally assess the use of hydrothermal media for dissolution of woody biomass. This project is just the initial step in the development of a two steps liquefaction process for aimed to obtain of bio-oils from bio-material.

Keywords: Bio-energy, Bio-refinery, Bio-Fuels, Hydrothermal liquefaction.

Introduction & Objectives

As result of the rapid growth of the global population and economies, a major issue in the modern society is finding solution that can satisfy the rapid increase of energy consumption. In the present, fossil non renewables resources are not only the main energy source used by humans, but also they are key raw material for the production of chemicals, fuels and even food. However, in the view of an imminent depletion of petroleum reserves, as well as on the need of finding a clean, renewable and carbon-neutral way of satisfying current human needs, biomass has recently become of major interest.

From the different technologies for the conversion of biomass into a source of energy, Hydrothermal Liquefaction (HTL) is a clean and promising technology that can be used to convert organic material directly into liquid fuels and other valuable compounds. This technology uses water in subcritical conditions as reaction media and reactant, therefore, it is very suitable for using wet biomass feedstock as algae or agricultural waste. Moreover, the process can also be used to pretreat biomass for bioethanol, hydrogen and methane production via anaerobic digestion.

Specifically, in the field of liquid synthetic fuels and biofuels production, HTL processes offer many advantages if compared with other technologies. For instance, HTL processes eliminate both the gasification step and the use of expensive catalyzers needed in the Fisher Trospsh process, reducing at the same time the temperatures required by to accomplish the energy conversion. But not only this, hydrothermal treatments also prevent the energy expensive water drying process of gasification and pyrolysis techniques. Furthermore, if the result of the HT process is a two phase fluid, the process can also avoid high energetic treatments as distillation. Most importantly, the HTL process lead to obtaining fuels with less oxygen content, higher carbon conversion efficiencies, higher LHV, and better C:H ratios, than those obtained via fast pyrolysis, when a suitable bio-stock is used.

In despite of the big advantages of Hydrothermal Technologies, the process is still at an early stage and improvements in conversion efficiency and selectivity are still needed. One way of reaching these targets is by properly assessing and controlling the effects of temperature in the liquefaction process. Previous studies have shown, for instance, that the very fast heating rates that micro reactors offer lead to fuels of better quality, by means of improving selectivity of the process. However, when a micro reactor is to be used, bio-stock particles of very small size are required, and, from a practical point of view, direct grinding of biomaterial to such small particle sizes are not economically viable.

One way of taking advantage of the benefits of the micro reactors, using at the same time bio stock particles of large sizes, is to use a two-step liquefaction process in which large particles are dissolved in water at subcritical conditions, and afterwards liquefied in a micro reactor. This innovative two steps process simplify the problems that many researches have had with regards to the feeding of hydrothermal systems.

In order to develop a brand-new liquefaction process of high efficiency and selectivity, the Norwegian University of Science and Technology acquired a brand new continuous liquefaction system that allows both liquefaction and gasification of biomaterial in hydrothermal conditions. Nevertheless the huge capabilities of this new system, some modifications are required in order to enable the two steps liquefaction process. In this context, the main objectives of this thesis work are:

a) Install the brand new PARR continuous flow tubular reactor system available at Thermal Lab and carry out comprehensive performance tests of the new system

b) Design, modify, develop and construct a continuous flow tubular reactor for hydrothermal dissolution of biomass, according to a two steps liquefaction process, followed by performance tests at temperature within 200-300°C.

c) Use the developed system to study the dissolution process of Norwegian Spruce, towards a future implementation of a two-step liquefaction process.

Based on these objectives, this thesis is composed of the following 4 chapters:

- In Chapter 1, a literature review including information about hydrothermal liquefaction processes is presented.

- In Chapter, 2 a description of brand new Parr system and the results of its performance tests are given. This chapter also includes a detailed step by step description of the analytical and practical procedures that were carried out along the development of the new dissolution system, as well as the results of its performance test.

- Chapter 3 is dedicated to show all the results obtained from the study of the dissolution process with the developed system. In particular, the effects of temperature in the dissolution process are carefully studies and described.

- In chapter 4, on the basis of the results shown on chapter 3 final conclusions are formulated and possible improvements or further works are suggested.

Chapter 1. Literature Review

1.1. Biofuels

Biofuels are fuels derived from biological renewable sources that contain energy from geologically recent carbon fixation. In general, biofuels can be in solid, liquid or gaseous state. Solid biofuels are mainly used for thermal energy applications via direct combustion. Examples are: dry wood, wood pellets, torrefied biomass and bio char. Liquid biofuels are aimed to replace conventional diesel and gasoline fuels in the transportation sector. Biodiesel, bio-ethanol and Fischer-Tropsch synthetic oils are available today, and in most cases, they are profitable alternatives to traditional liquid fuels. Finally, technologies such as gasification and anaerobic digestion produce valuable gas fuels as syngas or hydrogen from a wide spectrum of bio feedstock materials such as lignocellulose or agricultural and domestic wastes.

Liquid biofuels are classified into generations, according to the feedstock and to the process they use. In general they are classified as follows:

a) First generation Biofuels: They are produced directly from food crops by abstracting the oils for use in biodiesel or producing bioethanol through fermentation [1]. Crops such as wheat and sugar are the most widely used feedstock for bioethanol while oil seed rape has proved a very effective crop for use in biodiesel. However, the use of food crops for production of biofuels has been increasingly questioned due to the fact that they has contributed to the increase of the global food prices in the recent years. In addition, it has been proven that some biofuels can produce negative Net energy gains, releasing more carbon in their production than their feedstock's capture in their growth.

b) Second Generation Biofuels: Second Generation biofuels are produced from non-food crops such as wood, organic waste, food crop waste and specific biomass crops, therefore eliminating the "food vs fuels" problems [1]. Second

Generation biofuels are also aimed at being more cost competitive in relation to existing fossil fuels [2]. In addition, life cycle assessments of second-generation biofuels have also indicated that they will increase net energy gains over coming another of the main limitations of first generation biofuels. In particular, the use of lignocellulose material as raw material is very attractive as long as it is the most abundantly available raw material on the Earth. In fact, there exist several different processes that allow for the production of biofuels from this material. Figure 1.1. Illustrate diverse pathways for the production of second generation biofuels.

c) Third Generation biofuels: The Third Generation of biofuels is based on improvements in the production of biomass. It takes advantage of specially engineered energy crops such as algae as its energy source. The algae are cultured to act as a low-cost, high-energy and entirely renewable feedstock. It is predicted that algae will have the potential to produce more energy per acre than conventional crops. Algae can also be grown using land and water unsuitable for food production, therefore reducing the strain on already depleted water sources. [3].
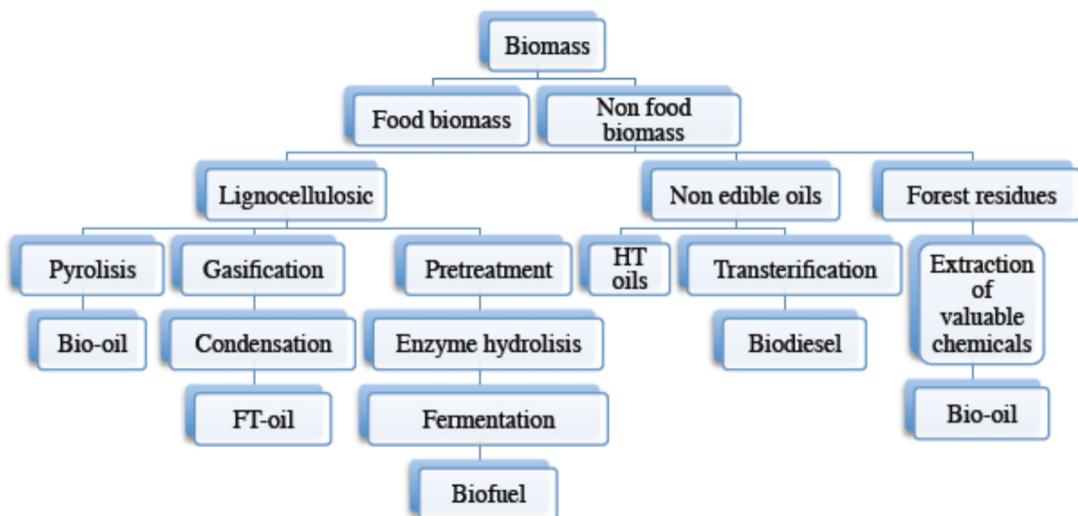
Figure 1.1 Possible pathways for transformation of biomass

1.2. Liquid biofuels production in hydrothermal media.

Hydrothermal technologies are broadly defined as chemical and physical transformations in high-temperature (200–600 C), high-pressure (5–40 MPa) liquid or supercritical water. This thermochemical means of reforming biomass may have energetic advantages, since, when water is heated at high pressures a phase change to steam is avoided which avoids large enthalpic energy penalties [4]. When the biomaterial is treated in the lower temperature range (200–400 C), the process mostly produce liquid products, often called "bio-oil" or "bio-crude", therefore the process receives the name of Liquefaction. Gasification processes generally take place at higher temperatures (400–700 C) and can produce methane or hydrogen gases in high yields. In general, hydrothermal processing can be divided into three main regions, liquefaction, catalytic gasification, and high-temperature gasification, depending on the processing temperature and pressure are shown in the Figure 1.2.
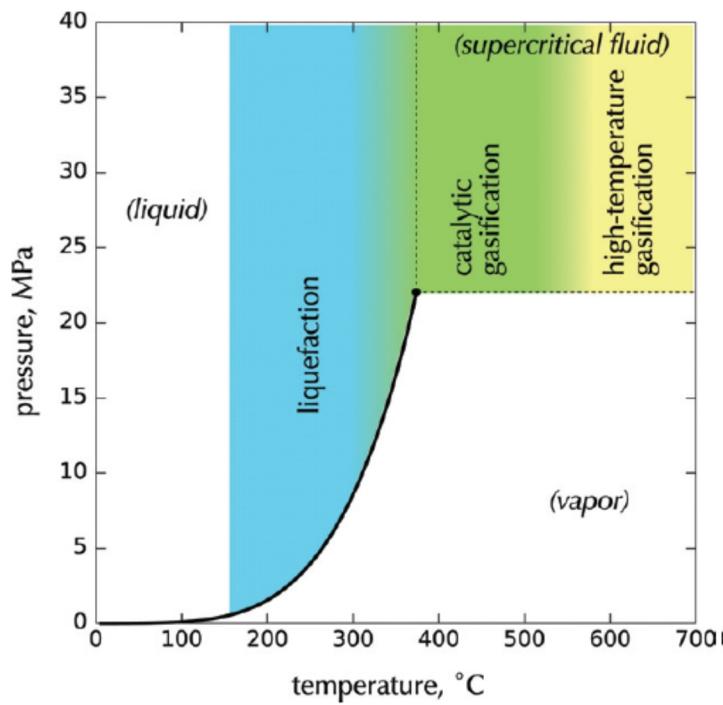
Figure 1.2. Hydrothermal Processes in P vs T Diagram

One major advantage of using hydrothermal media for the processing of biomasses is that it can act both as solvent and reactant in the reforming process of the biomass [5]. But not only this, using the fact that the physical properties of water near its critical point vary significantly with temperature and pressure, selectivity of the process can be controlled just by modifying the operative conditions of the process. This in particular occurs because near to its critical point, that biomaterials increase their miscibility with water, therefore improving the mass transfer in the reaction system. In addition, near critical water also improves its ability to sustain ionic and free radical reactions as long as the ionic disassociation of water reaches it maximum around 300 DegC.

The removal of oxygen from fuels derived from biomasses is a major objective, as removal of oxygen represent an improvement in the heating value of the fuel. Generally speaking, biomasses contain 40−60 wt% oxygen and conventional fuels and oils typically have only trace amounts, under 1%. Oxygen removal occurs most readily by dehydration, which removes oxygen in the form of water, and by decarboxylation, which removes oxygen in the form of carbon dioxide. These two removal mechanisms are highly exegetically efficient because both, water and carbon dioxide are fully oxidized and have no residual heating value, therefore accomplishing the task of removing oxygen major losses of the heating value. [5]

1.3. Lignocellulose Biomass and its reactions in hydrothermal conditions

Lignocellulosic materials constitute the bulk of the dry weight of woody and grassy plant materials, and as such are amongst the most abundant biochemicals on earth. Lignocellulose is composed of three primary components: cellulose, hemicellulose, and lignin; each of them behaving quite differently in hydrothermal conditions.

1.3.1. Cellulose.

Cellulose, like starch, is a polysaccharide composed of units of glucose connected via b-(1/4)-glycosidic bonds, which allows strong intra- and inter-molecular hydrogen bonds to form, and makes them crystalline, resistant to swelling in water, and resistant to attack by enzymes. Water at elevated temperatures and pressures can both break up the hydrogen-bound crystalline structure and hydrolyze the b-(1/4)-glycosidic bond, resulting in the production of glucose and fructose monomers. However, hydrothermal treatment of cellulose inevitably lead to further decomposition of the glucose monomers to decomposition products.

In general, it is commonly agreed that glucose degrades mostly to fragmentation products such as glycolaldehyde, pyruvaldehyde, glyceraldehyde, etc, [6][7][8][9][10], while fructose will react to a higher amount of the dehydration product 5-hydroxymethylfurfural (5-HMF) [11][12]. A detailed and complete pathway for the dissolution and decomposition of cellulose in hydrothermal media has been recently given by Cantero et al. [13] in his study. Figure 1.3 shows in detail such reaction pathways.
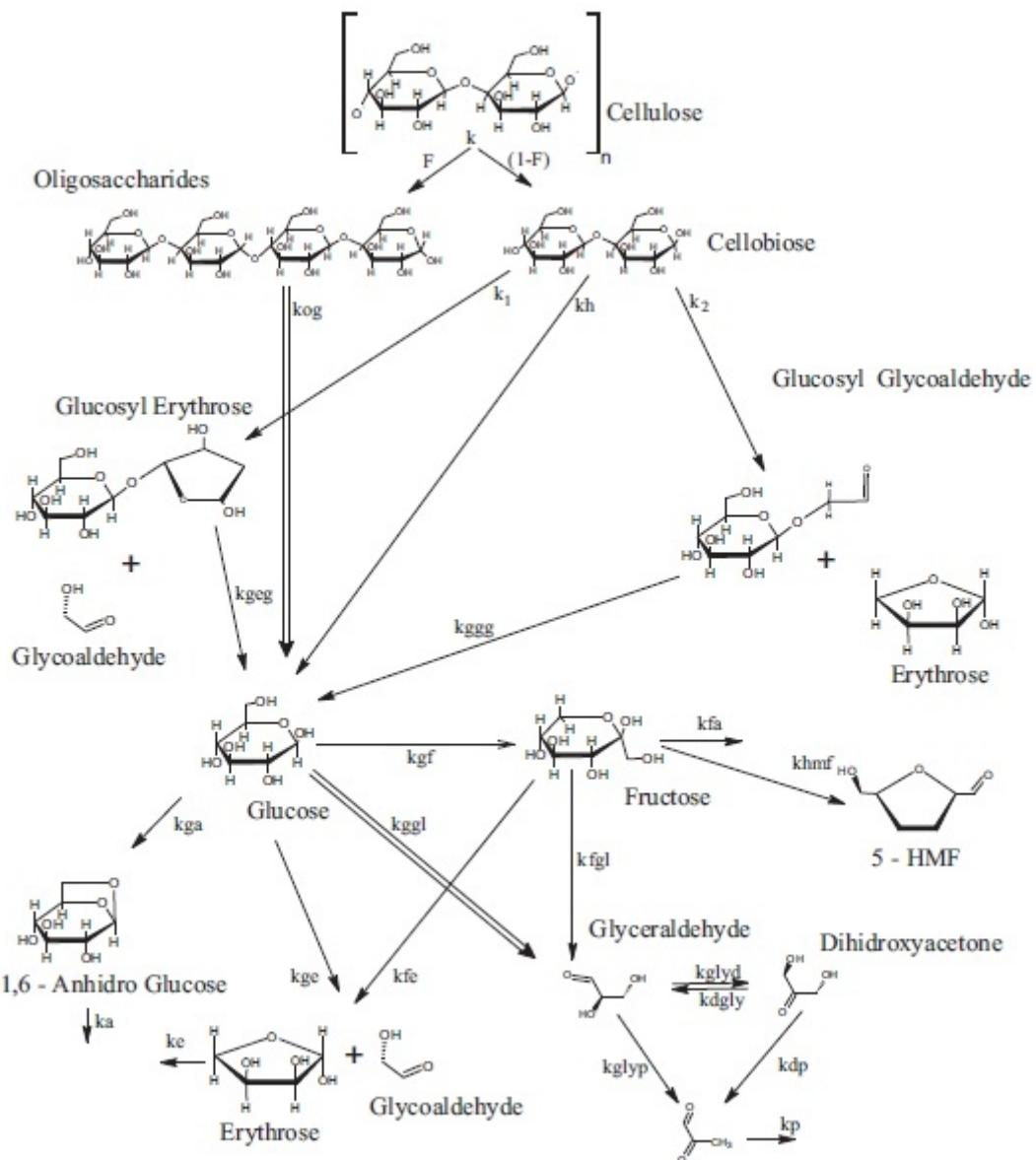
Figure 1.3. Hydrothermal decomposition of cellulose in hydrothermal media.

Regarding to the Kinects of this process, many authors have studied the decomposition of cellulose premixed with water in continuous flow reaction systems [14][15][16][17][18]. The best-fit line is fit to all of the data in Figure 1.4., from which an activation energy of 215 kJ mol is obtained.
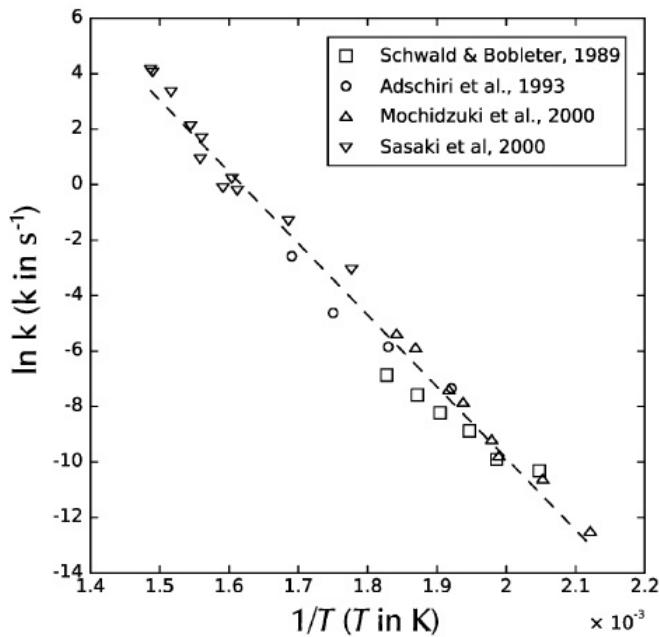
Figure 1.4. Arrhenius plot of natural logarithm of pseudo-first-order

1.3.2. Hemicellulose

Hemicellulose is a heteropolymer composed of sugar monomers, including xylose, mannose, glucose, galactose and others, which can also have side chains. The ratios of these monomers can change quite dramatically for different feedstock sources. Given the lack of repeating b-(1/4)-glycosidic bonds and the random nature of the hemicellulose polymer, it does not form as crystalline and resistant of a structure as cellulose does, and thus is much more susceptible to hydrothermal extraction and hydrolysis[4]. Extraction of hemicelluloses with efficiencies of up to 95% as monomeric sugars at 34.5 MPa and 200 to 230 DegC over a span of just a few minutes has been reported.[19][20]. A proposed kinetic pathway for the dissolution of the hemicellulose was proposed by [21] and is reported in the Figure 1.5.
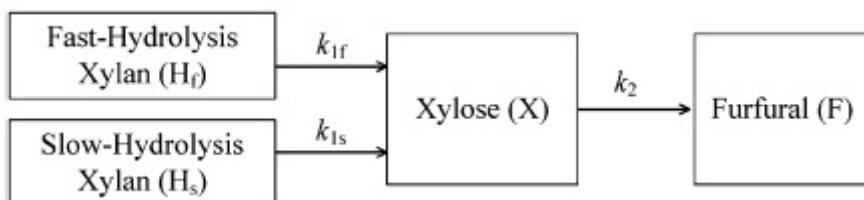
Figure 1.5. Kinetic Pathway for the depolimerization of Xylan.

1.3.3. Lignin

Lignin is a complex high molecular-weight compound with an even more random structure than hemicellulose. Lignin, which is a primary component of wood biomass, contains many oxygen-based functional groups, such as phenol, hydroxyl, carboxyl, carbonyl, ether and ester groups [22]. A number of researchers have explored using hydrothermal processes to extract potentially valuable chemicals from lignin as well as for oil production. For instance, at temperature ranges of 250-400 DegC, phenolic oils can be obtained via demethoxylation and alkylation of Lignin [23]. The density of water within the hydrothermal media has been found to be a key parameter. It has been found that higher water densities increase the breakdown of lignin for the production of oils and gases, presumably by enhanced hydrolysis with the higher water density. Regarding to its kinetic study, Wahyudiono et al [24] studied the degradation of lignin, using Guaicol as a model component. Furthermore, proposed pathways for the liquefaction of biomass have been proposed by many researches [25][26] , and they are shown in the Figure 1.6.
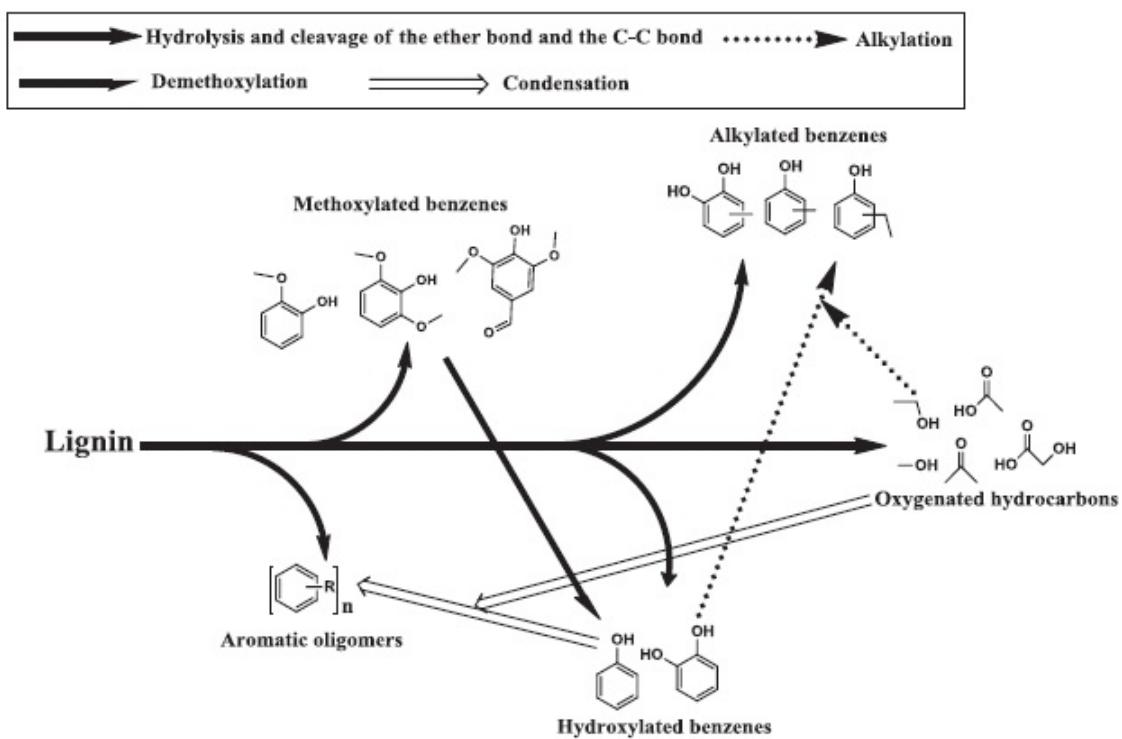
Figure 1.6. Kinetic pathways for dissolution of lignin.

Chapter 2. Liquefaction System Development

2.1. The Continuous Flow Reactor Parr-5401

2.1.1. Description of the system

The brand new 5401 continuous flow reactor system from Parr Instruments Inc., is a device that depending on its configuration and set up, can be used for diverse applications and research purposes [27]. In particular, the system owned by NTNU, can be used for processes where chemical reactions lead to products in gas and liquid phases. The system, as received, can be divided in 6 nodes as follows:

1. Gas Feeding
2. Water Feeding
3. Pressure control Node
4. Reactor and Furnace
5. Cooling Node
6. Separation and Collection node.
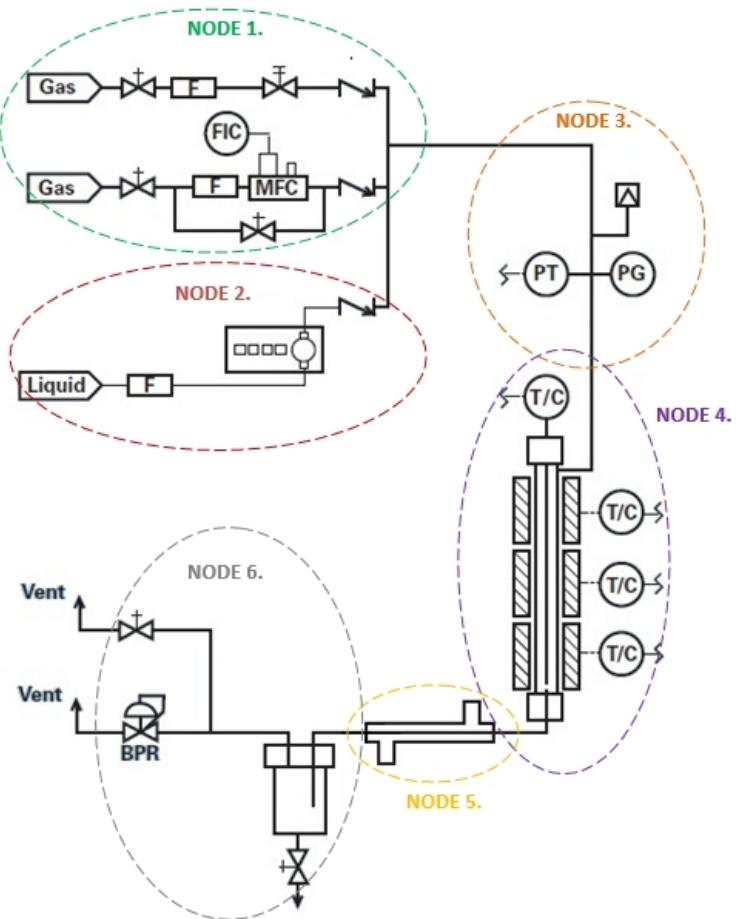
Figure 2.1. Continuous Flow System PARR 5401.

2.1.1.1. Gas Feeding

The first node is constituted by two gas lines for feeding the reactor. While line number one is designed specifically for Nitrogen supply, line number two can be used to feed the system with any gas.

Line number one (Nitrogen Supply), is enhanced with a Mass Flow Controller (MSC) BROOKS Delta II, able to provide Nitrogen to the system up to pressures of 300 Bars with a 100 bar pressure difference across de device. Line number one also offers the possibility of by-passing the MSC when needed. Additional instrumentation as check valves calibrated at 1 psi and stainless steels in-line filters of 0.7 um complete the instrumentation of the line.

On the other hand, line number two can be connected to any gas reservoir (N2, CO2, O2, CO, etc...), and the supply is controlled by means of a metering valve. Line number two does not offer the possibility of by-passing the valve, but it is also enhanced with the same additional instrumentation that line one has (check valves and filters).

2.1.1.2. Water Feeding

Water feed to the system is performed through a single tubing line of 1/16", at which only one pump can be connected. The system owned by NTNU have 3 different HPLC pumps that can be attached to this feeding line. The selection of the pump is given according to pressure, flow rate and precision needs. Each reciprocating pump can provide a constant water flow at different pressure conditions. Table 2.1 shows the differences between the three pumps.

Pump	Flow Rate [mL/min]	Max Pressure [psi]	Flow Resolution [mL]	Pressure Meter	Overpressure Control
1	0-10	4000	0.01	No	Yes
2	0-40	1500	0.1	No	Yes
3	0-100	4000	0.1	Yes	Yes

Table 2.1. Main Pump Characteristics

2.1.1.3. Pressure Control Node

The pressure control Node is located at the top of the system, just before the inlet of the reactor, and it is point where the three feeding lines meet. A pressure gauge, a digital pressure transducer and a safety rupture disk are installed in this point. The electronic transducer is connected to the Temperature controller Parr 4838, and from there the pressure in psi is visualized. The presence of these elements imposes some restrictions such as:

1. Pure oxygen cannot be used. This restriction is imposed by the materials the pressure transducer is made of.

2. It must not exceed the 85 Degrees Celsius.

3. While the pressure gauge and the pressure transducer can withstand pressures over 5000 psi, the rupture disk is calibrated to break down when the pressure of the systems overpass the 4500 psi.

2.1.1.4. Reactor and Furnace

The continuous reactor is a Stainless-Steel 316L tube with ID 0.28", OD 0.38" and a longitude of 24". The reactor is placed inside a 3-zone tubular furnace able to reach a maximum temperature 800 Degrees Celsius in each zone. The temperature of the reactor is controlled by means of three thermocouples inserted through the Furnace walls, in such a way that each thermocouple tip is in contact with the surface of the reactor. The geometrical location of these thermocouple holes is exactly the centre of each zone of the reactor.

The reactor is also enhanced with a thermo well that allows the introduction of a thermocouple in the radial centre of the reactor, allowing the measurement of the internal temperature at any length of the reactor.

The temperature control is carried out by connecting the thermocouples to three PID controllers Parr 4838. A detailed scheme of the geometry of the furnace and the reactor are given in the Figure 2.2..
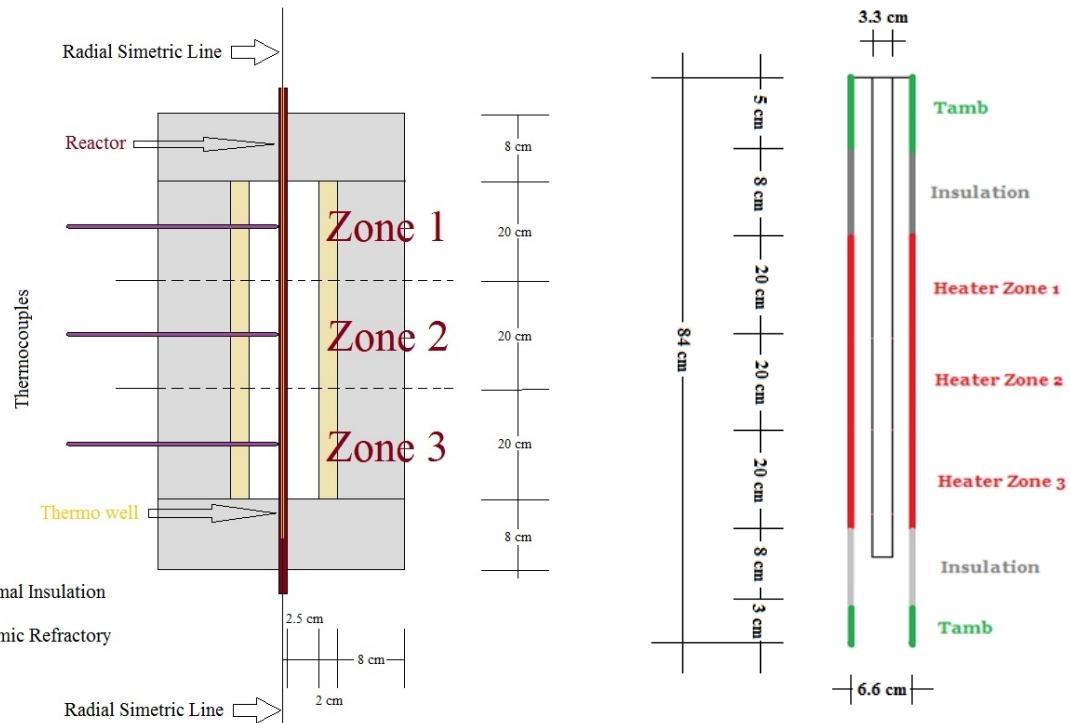
Figure 2.2. Left: Furnace arrangement. Right: Reactor and Thermo well Geometry

2.1.1.5. Separation and Collection nodes

Following the tubular reactor, a cooling jacket has been installed. If the reactions took place in gas phase, formation of condensates is expected when the stream passes through this heat exchanger. For this reason, a collection vessel of 0.6 Litters (Ref. Parr 4615) is located immediately after the cooling jacket. While a metering valve is placed in the bottom of the vessel for liquid samples collection, in the top of the vessel, the venting line and the BPR lines are located.

The most important element of this node is the Back Pressure Regulator, located on the vessel´s gas outlet line. By means of this element, the pressure of the whole system is kept constant at a given set point in a range from 0 to 300 Bar. It is important to outline that the BPR cannot be subjected to streams with temperatures higher to 85 DegC.

More information about safety and operation conditions can be consulted in the Rig dossier prepared for this device. In the dossier, the risk assessment and the data sheet of all the elements that constitute the system can be found.

2.1.2. Risk Assessment

By safety regulations of the NTNU Thermal Lab, it was required to develop a risk assessment for the new liquefaction system. In this document, following the guidelines for developing HAZOP studies, the system operator makes a global analysis of the system, identifies risks sources and formulate solution for possible issues that might arise when running experiments. Furthermore, the assessment must include a detailed step by step guide for carrying out experiments, as well as the required procedures an actions to be taken in case of emergency situations. The developed risk assessment is left in the technical documentation pocket of the rig, in the Thermal Lab.

Immediately after approval of the risk assessment, assembly and test of the system were carried out as described in the following sections.

2.1.3. Assembly of the system and testing of components.

The system was received in two big boxes. All pieces and components were properly marked for assembly, but neither guidelines nor schematics of the system where provided. However, supported on the marking of the elements and on the schematic given in the Figure 1, (obtained from an online brochure), the system was successfully assembled. Before starting with any experiment, datasheets of all the components in the system were downloaded and read (pumps, valves, vessels, filters, BPR, etc.).

The testing of the system was organized in three sets of experiments. The first was focused in the furnace, where a temperature test was performed. The second evaluated the behaviour of the system when subjected to high pressures. Finally, the last set of experiments was the characterization itself of the whole system. Each test is explained carefully in the following sections.

2.1.3.1. Temperature Tests:

At first stage, the empty furnace (No reactor inside) was tested in the range of 100 to 750 Degrees Celsius (Maximum Temperature is 800 DegC). The testing methodology was based on a temperature swept from 100 to 750 DegC, in increments of 50 DegC. For each increment, the furnace´s temperature was kept constant for at least 30 mins after stabilization at the set point.

After completing the temperature swept, the temperature was decreased to 450 DegC, and the furnace was held at this state for 4 hours.

2.1.3.2. Pressure Tests:

To perform the pressure tests, a Nitrogen Tank was connected to the Gas line number one of the system. Having into account that a precise control of the amount of gas entering into the system was not required for these experiments, the gas flow was controlled manually through the tank´s Pressure Regulator and not by means of the Mass flow controller, which, in fact, was by-passed.

The test started by setting the Back Pressure Regulator at zero pressure, and the tank´s regulator 50 bar. This condition generated a fast discharge of nitrogen from the bottle to the atmosphere (through the venting line of the system), that was slowly controlled by tightening the Back Pressure Regulator. When the BPR was sufficiently closed to stop the flux of Nitrogen, the inlet valve of the gas line was closed and the system was held at this state. After one hour, the pressure was increased to 100 bar, and the system was kept at this state for another hour. This procedure was performed 4 times, for pressures of 50, 100, 150 and 200 bar.

With this methodology, not only the behaviour of the BPR was evaluated, but also, the presence of leakage in the system was evaluated. For instance, at pressures of 150 Bar and above, a very little (almost negligible) leakage was present. Such leaked was identified by means of the electronic pressure transducer, and it was equivalent to pressure losses of about 1 - 3 psi/min.

2.1.3.3. Pumps testing:

Testing of the pumps consisted in a Flow rate swept at three different pressure levels (atmospheric, mid-range and maximum pump's pressure). Regarding to the flow rate, water injections were performed at 5 fixed points covering the whole operative range of each pump.

In this sense, for the Pump 1 (10 mL/min), the system was pressurized at 0, 125 and 250 Bar, and water injections performed at flow rates of 2, 4, 6, 8 and 10 mL/min. For Pump 2 (40 mL/min), the system was pressurized at 0, 50 and 100 Bar, and the water injections performed at 8, 16, 24, 32, and 40 mL/min. Finally, for the third pump, same pressure as pump one were established, but water flow rate injections were made at rates of 20, 40, 60, 80 and 100 mL/min. This information is summarized in Table 2.2.

PUMP	PRESSURE [Bar]	FLOWRATE [mL/min]
	0	2,4,6,8,10
Pump No 1	125	2,4,6,8,10
	250	2,4,6,8,10
	0	8,16,24,34,40
Pump No 2	50	8,16,24,34,40
	100	8,16,24,34,40
	0	20,40,60,80,100
Pump No 3	125	20,40,60,80,100
	250	20,40,60,80,100

Table 2.2. Pumps testing conditions

2.1.3.4. Practical Observations and recommendations

Some important conclusions were obtained from these experiments:

1. When pumps work at a pressure higher to that of its maximum operative condition, they can either, be shut down for the protection mechanism, or produce strange noises. In general, the shout down mechanism is self-activated when pumps experience fast pressure increases, but they produce abnormal noises when the pressure slowly goes over its limiting value. In fact, this behaviour was specially observed in pump number two.

2. Despite Pump No 3 (100mL/min) is designed to work up to pressures of 275 Bar, it was found that the Pump was not able to provide its maximum flow rate at pressures over 200 Bar. At pressure levels over 220 bar, abnormal noises were produced when water flow rate exceed the 85 mL/min. Based on this behaviour, all the experiments carried out in this work where limited to a flow rate of 80 mL/min, when using the pump number three.

3. It is possible to obtain pressures over 200 bar by means of an initial pressurization with nitrogen, followed by a compression of the gas pre-loaded by means of injection of water injection to the system. Using this technique it was possible to reach pressures of up to 300 Bar.

4. Another abnormal operative condition of the pump occurs when suddenly it stops the water injection, but no activation of the overpressure mechanism is activated, nor abnormal noises are produced. This situation is easy to identify just by looking at the container from where the pump is suctioning water. If the level does not decreases accordingly to the water injection flow rate, the pump is working abnormally. If this conditions occurs, purging (as described in the manual of the pump) is required. As general tip, cylindrical containers of small diameter and high capacities suit the best as pumps reservoirs. A total capacity of at least 2 Litters is advised.

5. It is very important to pay special attention to these events, because it can happen that the pump goes into a state of no flow condition while its overpressure mechanism is not activated. This condition is especially dangerous for the integrity of the pump and it must be always avoided. From experience, after 6 months working with this HPLC pumps, it was observed that

the pump always activates the shout down mechanism by over pressure when at a fixed flow rate, the system experience a rapid increase of pressure, as in the case of pressurization by both, nitrogen and compression by water.

2.2. The Parr system and the hydrothermal liquefaction processes.

2.2.1. System limitations

In the recent years, most of the research in hydrothermal liquefaction of biomass in continuous flow has been carried out using systems where:

1. A slurry of organic compounds (mostly cellulose or glucose), is mixed up with pre-heated water (in subcritical and super-critical conditions) .
2. The mixture enters into an adiabatic tubular reactor, where the liquefaction take place.
3. After reaction, the stream is cooled down by either, a cooling jacket, or by mixing the main fluid stream with cold water.
4. Finally, the cold stream passes through a Back Pressure Regulator and samples are collected.

An overview of a traditional liquefaction system is given in the Figure 2.3.
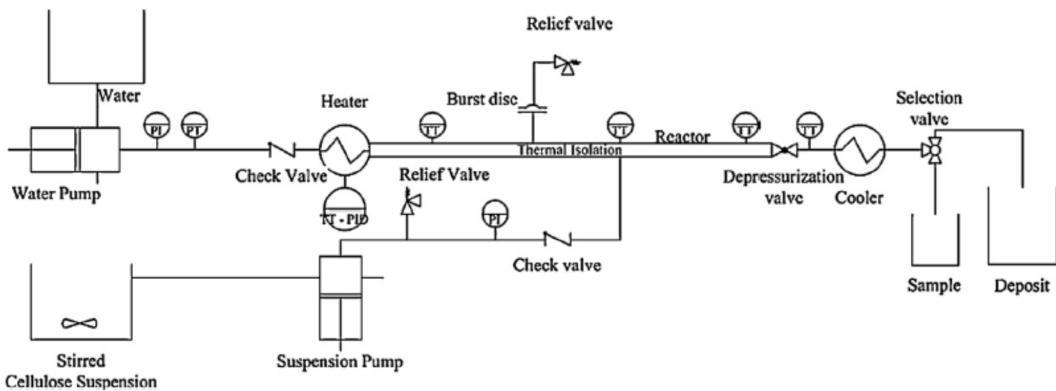
Figure 2.3. Traditional Continuous Flow Set up for liquefaction experiments. [13]

The Parr system, as delivered, is suitable for hydrothermal liquefaction experiments where pre-mixing of the organic slurry with subcritical water is not required. According to Figure 2.1, in the Parr system the slurry is directly injected into the reactor, where it is rapidly heated up and further reacted. However, there are some issues related with this type of setup. Firstly, this configuration has to guarantee that the stream is rapidly heated in a short length of the reactor, then leaving most of its volume for the reaction itself. In other words, the addition of the heating time and the reaction time has to be equal to the total residence time of the stream in the reactor. Secondly, there exists a big limitation in the type of material to be injected with the HPLC pumps, as long as they are not designed for handling fluids of high viscosities, or with particle sizes bigger to 0,7 um. Keeping in mind these limitations, as well as the fact that this study is focused on liquefaction processes of woody biomasses, it is obvious that the system needed some modifications.

To overcome all the mentioned problems, it was planned to use the Parr reactor as a fixed bed reactor in semi continuous flow conditions, where biomass would be pre-loaded, treated, and then the process stopped. The semi continuous operation implies that for every run, the reactor should be opened, cleaned and re-loaded, re-pressurized and re-heated.

The feasibility of this liquefaction technique is evaluated mainly by three factors; some of them already mentioned:

1. The amount of biomass that can be placed inside the reactor.

2. The heating rate of the device
3. The temperature profile inside the reactor.

2.2.1.1. Amount of Biomass loaded into the reactor:

The amount of biomass that should be loaded inside the reactor must be as large as possible to avoid any problem with mass balances. In this sense, the amount of biomass needed is directly proportional to the flow rate of water pumped into the system, the more water pumped into the system, the more biomass is needed in order to increase the concentration of organic compounds in the resulting solution. The total amount of biomass required by the experiment is also determined by the analysis technique (TOC, HPLC, GC-MS, or others) to be used. As general rule, a concentration of 1 gram of organic compounds per Kilogram of water is advisable.

A second variable to keep in mind is the relative volume occupied by the biomass. This volume mainly depends on the grain size of the biomass. To evaluate this parameter, two samples of woody biomass, one with a chip size of 2 mm, the other with very small grains of 90um (both of them dried overnight at 105 DegC), were placed in a small containers of 100 mL, then, with the help of an electronic scale of 0.001 mg accuracy, the mass of the sample in the container was measured. The results of this experiments are summarized in the next table:

Chip size	Mass in a space of 40 mL
90 um	16,39 gm
2 mm	12,56 gm

Table 2.3. Biomass Specific Volume

2.2.1.2. Heating Rate of the device:

The heating rate of the device should be as fast as possible in order to avoid premature depolymerisation and further reactions at temperatures lower than the target one. If the heating time of the device is too long or comparable with the reaction time of the biomass, it could happen that once the reactor has reached the target temperature, all

the biomass has already reacted. This phenomena has already been reported by Mosteiro-Romero et al. [28]. To diminish the probability of such undesired reactions, it is also required to have short stabilization temperatures. In fact, to obtain accurate results, the stabilization time should be much shorter than the reaction time. According to literature, hydrothermal liquefaction reactions can take between 10 and 40 mins.

2.2.1.3. Temperature profile inside the reactor:

In order to properly study the effect of the temperature in the liquefaction process, isothermal conditions must be guaranteed for the fluid flowing through the biomass loaded into the reactor. This condition implies that the biomass must be placed in a point where the thermal boundary layer has reached its full developed condition, therefore, the amount of biomass loaded into the reactor varies as the temperature profiles does. For instance, the volume available for biomass placement is reduced as the entry length of the thermal boundary layer increases.

The assessment of the boundary layer is firstly carried out theoretically by means of CFD and Matlab modelling, as well as experimentally. The full description of the procedures is given in the following sections.

2.2.2. Reactor Analytical Study

2.2.2.1. CDF Model of the reactor:

The simulation of the Heat Transfer phenomena was performed in a 2D Model using Comsol's Conjugate Heat transfer Module. The main hypothesis of the study was the assumption that the reactor had isothermal walls at the target temperature set in the temperature controllers. This isothermal condition was modelled only in 60 cm of the whole reactor surface (equivalent to the heating area of the furnace). Also, insulation and ambient temperature boundary conditions were imposed in the reactor walls matching with the reality. The materials included in this simulation were: Water, Air, and SS316 Polished; all of them included in the Comsol´s Libraries.

The main objective of this investigation was to find the distance at which the flowing water reached the target temperature. For the geometry given in the Figure 2, the simulation was performed for a reactor's wall temperature of 350 DegC and a water flow rates of 1, 5, 20 and 60 mL/min. Figure 2.4 shows the results of the simulation.
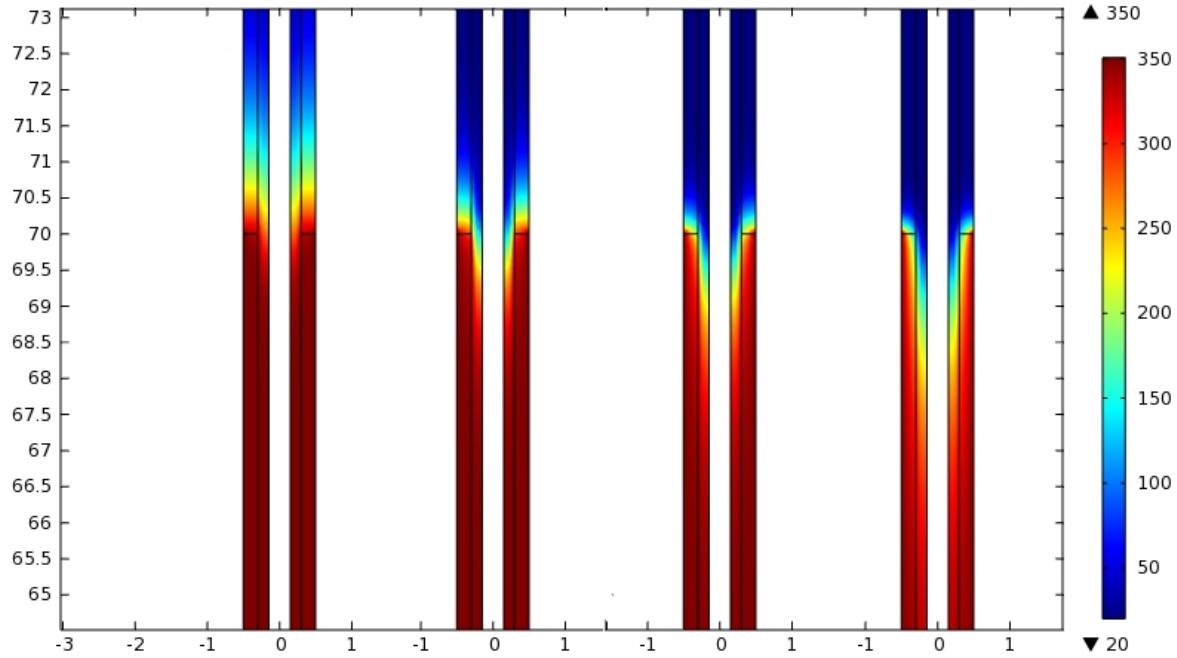
Figure 2.4. Temperature Profiles at 1, 5, 20 and 60 mL/min from left to right respectively.

Flow rate [mL/min]	Entry Length [cm]	Temperature [C]
1	1	345
	2	349
5	1	315
	3	345
	4	349
20	1	262
	3	332
	7	349
60	1	179
	3	288
	9	345
	14	349

Table 2.4. Temperature at different entry Lengths and flow rates.

The results of CFD model clearly show the effect of the flow rate in the temperature profile of the reactor. The slower the flow rate, the shorter is the entry length required to fully develop the thermal profile. It is interesting also to notice that as the flow rate is reduced, the upstream water and reactor temperatures increase. Some punctual measurements from this study are summarized in the Table 2.4.

2.2.2.2. Matlab Simulation:

In order to confirm the results obtained with Comsol, a Matlab model was developed. The model was based on the assumption of convective heat transfer from an isothermal surface (reactor's wall) to a liquid flowing in laminar conditions. Reactor's wall temperature was fixed to 350 DegC, and water flow rate was studied at 1 and 5 mL/min.

The code was developed based on an iterative process that performed calculations on the energy equation inside the reactor. The model of the heat transfer is given in Figure 2.5, while the energy equation is given in (1).

$$\dot{Q} = h\pi D L \Delta T_{\mathrm{LM}}$$

T1   **T0**   T2

$$\dot{Q} = \dot{m}c_p(T_2 - T_1).$$

L
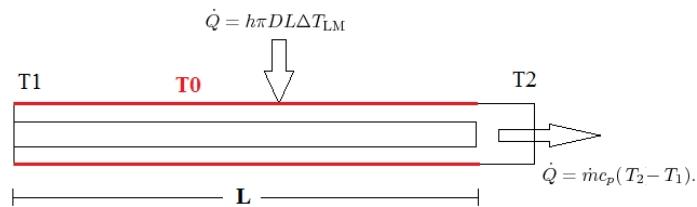
Figure 2.5. Reactor´s Heat transfer phenomena included in model.

$$\square \pi D L \Delta T_{LM} - \dot{m}c_p(T_2 - T_1) = 0 \quad (1)$$

where:

$$\Delta T_{LM} = \frac{T_2 - T_1}{\ln \dfrac{T_0 - T_2}{T_2 - T_1}} \quad (2)$$

The heat transfer coefficient h in (1), is given by the properties of the fluid and was calculated based in the well-known experimental correlations for heat transfer problems in laminar conditions [29].

The iterative process was tested using two different approaches from which the most efficient was selected. The first one, based on the Newton-Raphson iterative method to find the roots of a nonlinear equation, found the temperature at which the energy equation was satisfied for a specific reactor length. However, this method consumed plenty of computing resources, time, and presented many converging issues. In order to overcome these problems, instead of implementing an infinite loop with error evaluation as stopping condition, a finite loop that evaluated the energy equation for all the temperatures in the domain, from 0 to the reactor's wall temperature was performed (350 DegC in this case). Under this methodology, the length at which the energy equation evaluation is performed is an input parameter of the code.

After evaluating the energy equation at all the points, with a resolution of 1 DegC, the results were plotted and the solution was found by graphical approach. The Temperature at which the energy equation is satisfied at the length L, is the one at which Power in - Power out is equal to zero.
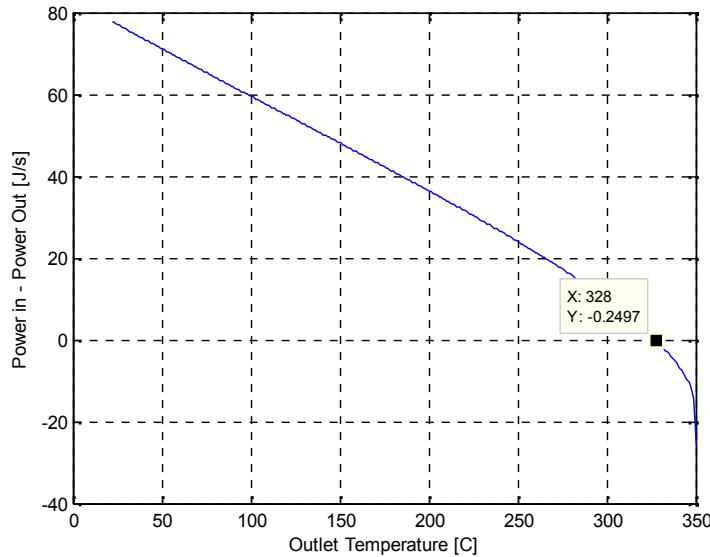
Figure 2.6. Energy Balance equation for 1 mL/min at 1 cm entry length.
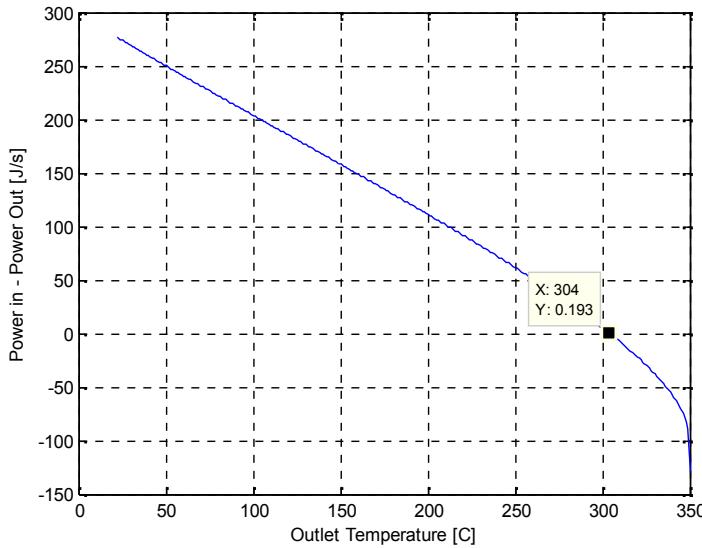
Figure 2.7. Energy Balance equation for 5 mL/min at 3 cm entry length.

The Figures 2.6 and 2.7 show clearly that the Matlab model predicted values that are slightly lower than the ones obtained via CFD simulation, therefore, the entry length required for reaching a fully developed state of the thermal boundary layer is larger in the Matlab code than in the Comsol's model.

2.2.3. Reactor Experimental Study

The performance test was carried with the objective of evaluating the system suitability for carrying out hydrothermal liquefaction experiments. With such aim, two different set of experiments were designed:

1. The first set of experiments studied the effect that Pressure, Furnace temperature, and water flow rate had over the temperature of the fluid leaving the reactor.
2. In a second set of experiments at target temperatures (200 – 380 DegC) and pressures (100 - 200 Bar), the temperature profile inside the reactor was studied.

2.2.3.1. Outlet Temperature Experiments

2.2.3.1.1. The methodology:

The methodology followed in this set of experiments consisted in splitting up the three dimensional problem into many problems of two variables. These two variable problems where then subdivided into many ones of one single variable, therefore facilitating the experimental study.

Before starting with the experiments, it was imperative to find both an appropriate domain of study and its discretization. The selected ranges for the multivariable study and the domains discretization are summarized in Table 2.5. All the values were selected having into account the required conditions for hydrothermal liquefaction processes.

Variable	Range	Domain Discretization
Pressure	50-250 Bar	50, 100, 150, 200, 250 Bar
Temperature	200-550 DegC	200, 250, 300, 350, 400, 450, 500, 550 DegC
Flow Rate	5-80 mL/min	5, 10, 20, 35, 55, 80 mL/min

Table 2.5. Domains Selection and Discretization parameters.

Once the domain and discretization points were selected, the idea behind the study was to set the main variable (pressure) to its initial value: 50 Bar. Then, the secondary variable (Temperature) was set also to its first value: 200 DegC. Finally, the study of the fluid temperature leaving the reactor was carried out for changes in the flow rate variable, starting from 5 mL/min, and ending up in 80 mL/min. Each of this set of experiments is called "a run".

Once the swept in the flow rate domain was concluded, or in other words, a run was completed, the furnace temperature was increased, and a new run was made. This process was repeated until the whole points in the temperature domain were covered. When the bi-dimensional problem flow rate – temperature for one pressure level was completed, the pressure was increased and the whole process repeated until the 5 pressure levels were covered. The results of the study are given in the next section.

2.2.3.1.2. Results

A total of 27 runs were made to complete the characterization of the reactor. In a day, two runs were made, therefore, in 14 days the characterization was completed.

At the beginning of the each day, the system was initially pressurized with Nitrogen of quality 5.0 up to the desired pressure (Pressure set point was fixed by tightening or loosening the BPR). After the pressurization step, water injection was performed and then, heating of the furnace started.

Before any experiment, the system was left for 6 hours until it reached its steady state. Following the stabilization time, the fluid temperature leaving the reactor was measured and registered. After taking the measurement, the water flow rate was increased, a new stabilization time was allowed and the next reading was taken. This process was repeated for all pressures and temperatures in the analysed domain.

A very important remark of this characterization is that it involved water injection into the reactor from the bottom and not from the top. The main reason for having changed the point of injection recalls to the fact that water injections from top do not guarantee a reactor full of water the whole time; in fact, it may happen that after pressurization, the water flushed through the system falls freely inside the empty the reactor, reducing significantly its residence time. Most importantly, not having the reactor full of water will significantly affect the liquefaction reactions. In fact, it might occur that biomass is treated in two different media, Nitrogen and hot compressed water, therefore affecting the reliability of the data obtained from the process.

The results of the characterization are given in the Figures 2.8 to 2.12. In each of the five figures (one per pressure level), the variation of the fluid temperature leaving the reactor is plotted against the water flow rate.
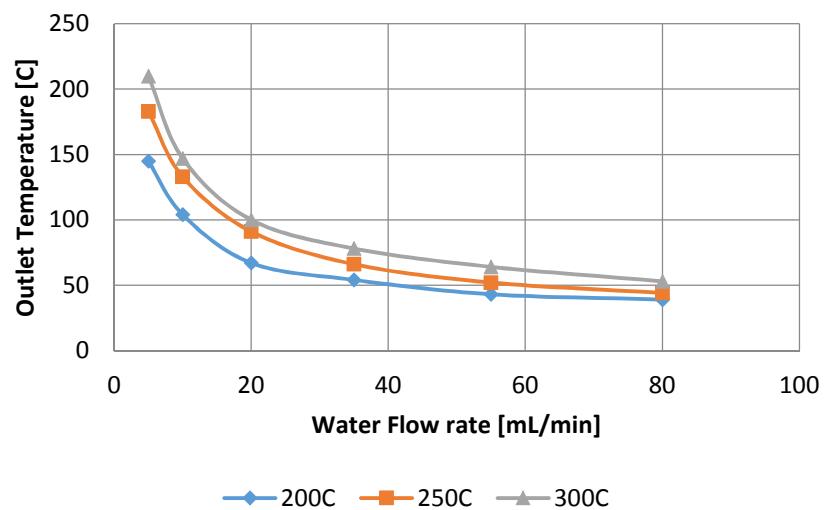
Figure 2.8. Outlet Water Temperature vs Water Flow rate at 50 Bar.
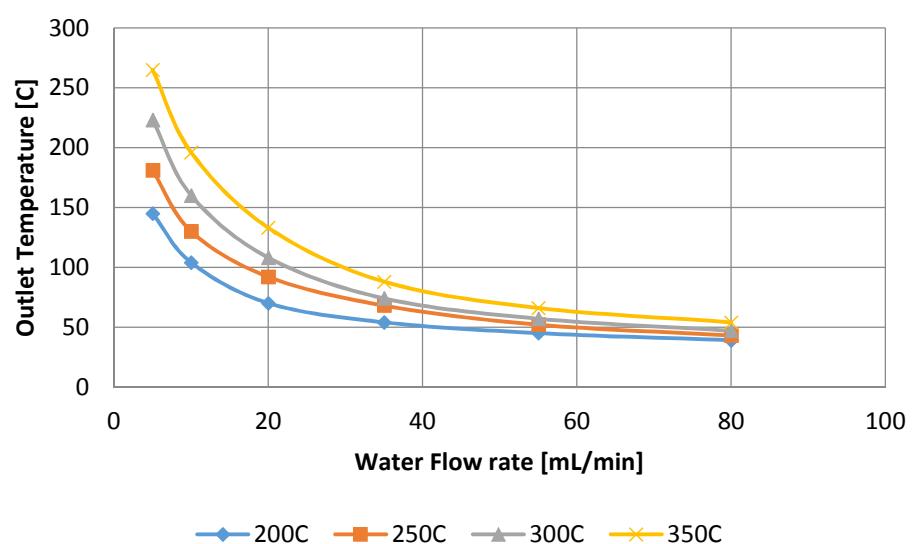
Figure 2.9. Outlet Water Temperature vs Water Flow rate at 100 Bar.
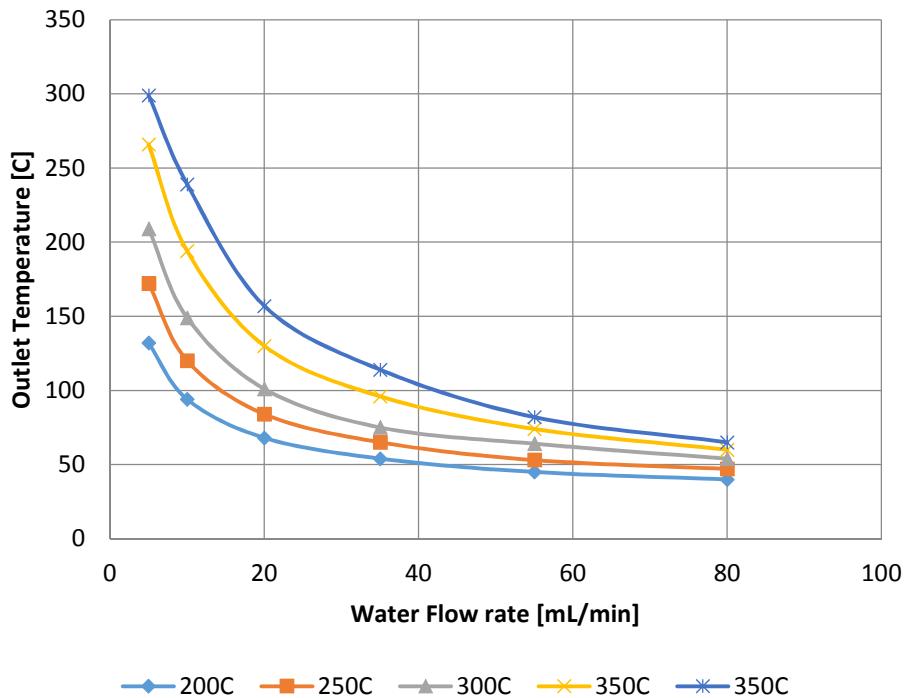
Figure 2.10. Outlet Water Temperature vs Water Flow rate at 150 Bar.
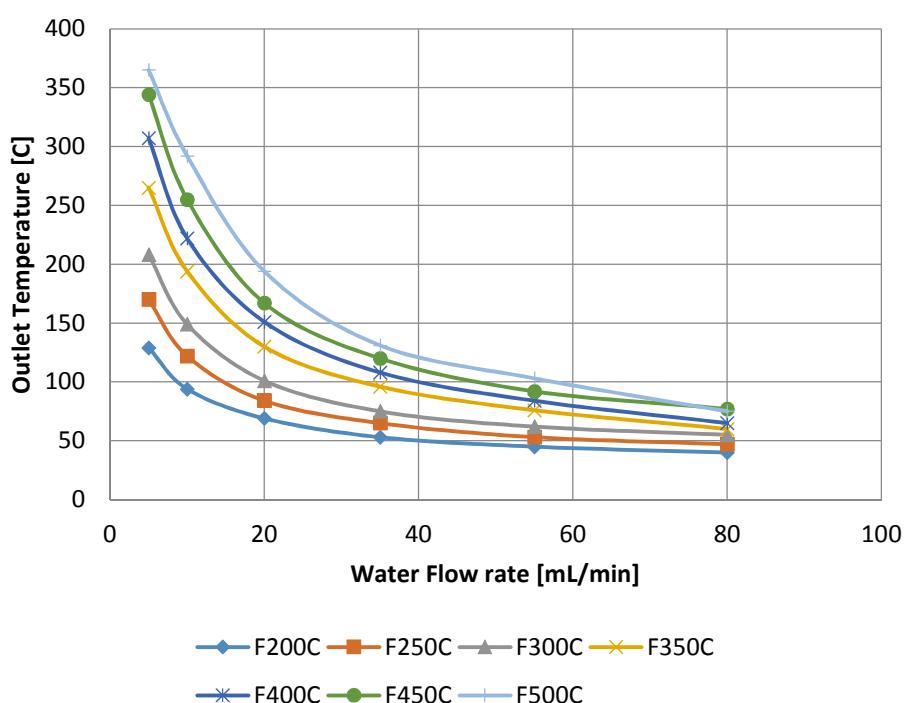
Figure 2.11. Outlet Water Temperature vs Water Flow rate at 200 Bar.
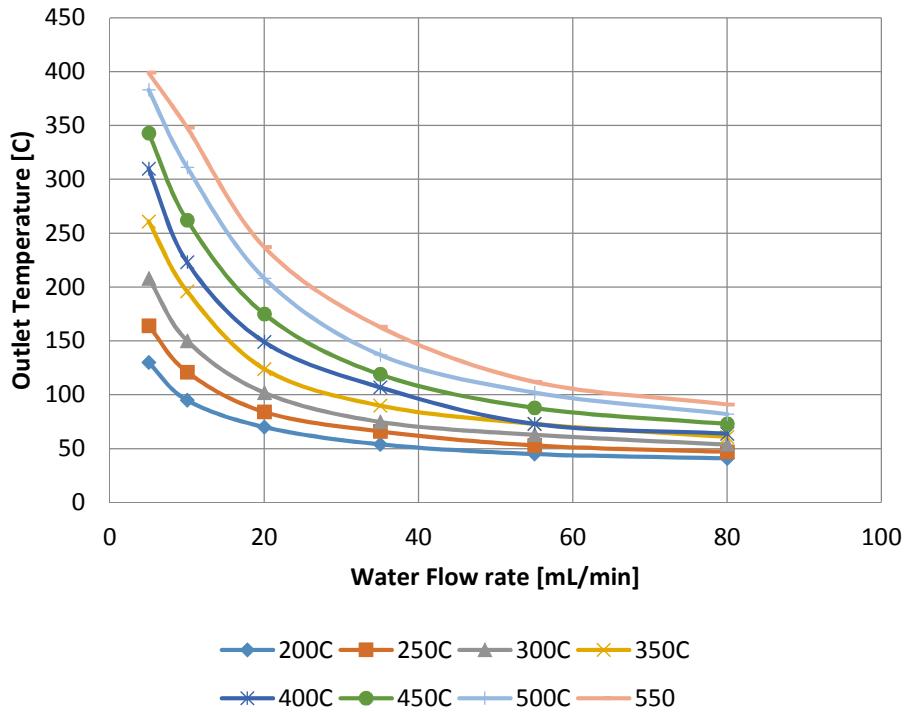
Figure 2.12. Outlet Water Temperature vs Water Flow rate at 250 Bar.

As it was expected, the results show that at fixed pressure and furnace temperature conditions, the outlet temperature decreases exponentially as the water flow rate increases. Another interesting observation is that the outlet temperature is not heavily affected by pressure variations. This means that for different pressure conditions, the Outlet temperature curve does not change considerably, neither in shape nor in its initial temperature. For instance, for a temperature of 300 DegC, the initial point is always located just above 200 DegC in all the figures. (The same occurs for all the other temperatures).

It is important to mention that for the previous experiments, the maximum furnace temperature was limited to the boiling temperature of the liquid. This limitation was imposed with the aim of avoid any phase change inside the reactor, therefore keeping the water always in liquid state.

The previous results also suggest that regardless the furnace temperature, liquefaction experiments at high flow rates cannot be carried out because the system is not able to raise the water temperature up to suitable process values. Also, according to these results, it is possible to conclude that at the maximum furnace temperatures

conditions, the maximum flow rate possible for liquefaction experiments in the PARR system cannot exceed the 20 mL/min.

On top of all what has been previously mentioned, the most important observation from these experiments is the huge disagreement between the real temperature reading and the ones obtained in the models. According to Comsol, even at 60 mL/min, a length of 20 cm is enough to bring the water to the set point, however, from Figures 6-10, it is possible to observe that at the temperature of the water leaving the reactor is only 65 DegC. This incoherence between model and experimental results makes obvious that the assumptions made for the initial model have to be reconsidered and a new model has to be built.

2.2.3.2. Temperature profile experiments

In order to obtain additional information that could help to verify the hypotheses that were made when the CFD model was developed, this new set of experiments traced the thermal development of the reactor along its whole length.

The temperature profile inside the reactor was studied for conditions of low and high volumetric flow rates. While for the low flow experiments (1 and 2 mL/min) a very detailed temperature profile was built (12 readings were taken to build up the profile), for the high flow experiments (5 to 55 mL) a less detailed study was carried out (3 points along the whole profile).

2.2.3.2.1. Methodology:

For the case of low flow conditions, the temperature profile was studied by taking measurements of the temperature inside the reactor along its whole length. The reference zero is arbitrary located at the point where the heating zone of the furnace starts and the last point is located 63 cm away from it. This last point coincides with the bottom of the thermo well inside the reactor. Eleven temperature readings were taken every 6 cm starting from the outlet of the reactor (the bottom of the thermo well), and the last reading was taken not at 6, but at 8 cm from the preceding point.

Regarding to temperatures, 350 DegC was selected as the as the main analysis temperature. The results of this experiment are summarized in the Figure 11. Despite that liquefaction experiments are carried out in the range of 200 to 400 DegC, with the aim of evaluating the behaviour of the system in case of evaporation phenomena occurring in the reactor, an additional experiment at 200 Bar and 600 DegC was also performed at low flow rates.

For the case of higher flow rates, the experiments were focused on making a fast assessment of the impact that the flow rate has over the temperature profile at different pressure conditions. This time, measurements at different volumetric flow rates (5, 10, 20, and 55 mL/min) were taken at only at three points inside the reactor: the first at the bottom of the thermo well (at 63 cm from the zero reference); the second at 20 cm from the first point (43 cm from zero), and the last one at 23 cm from the zero reference. The results are given in the Figures 2.13 to 2.17.

2.2.3.2.2. The Results:

After allowing a period of 6 hours for thermal stabilization of the system, the four experiments at low flow conditions were run. After completion of this first round, the experiments were repeated and a huge variability, respect to the first experiments was observed. To overcome the uncertainty about the results, a third round of experiments was carried out and the results showed a variability of +/- 3 DegC respect to the second round. The data reported in Figure 2.11 is the average between the results of the second and third runs.

In the same way that was observed in the outlet temperature experiments, the pressure effects over temperature are almost negligible. In fact, for 1mL/min and 350 DegC, the temperature profile for 150 and 200 Bar is almost the same one.

It is also interesting the fact that the temperature profile does not change much for 1 and 2 mL/min. However, the entry length for 1 mL/min is approximately 6 cm shorter than the one at twice the flow rate. On top of everything, it is noticeable that the heat losses present at the outlet of the reactor are the same for both flow rates. This hypothesis is based on the observation that after 50 cm, both temperatures profiles

reached the same maximum point and then they started to decrease at same rate, reaching the same outlet temperature.
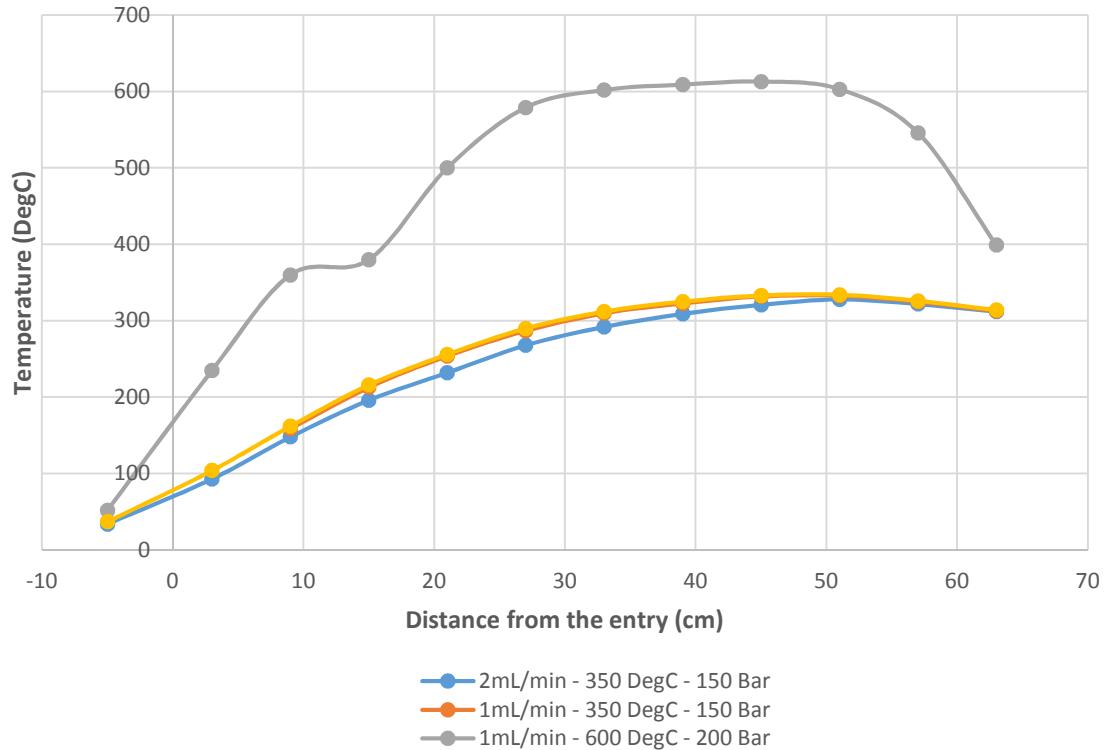
Figure 2.13. Water Temperature at Different Reactor`s Lenghts

For the experiment at 600 DegC, it is observed that the temperature profile can be divided in three sections were the compressed water is first heated up, then boiled, and finally, super-heated in gas phase. The behaviour of the first, second and third regions are respectively linear, then flat, and finally somehow parabolic. These behaviour can be explained according to the nature of the heat transfer phenomena occurring in each region, which are respectively: forced convection in liquid phase, phase change at constant pressure, and forced convection in gas phase. In the other hand, for the experiments at 350 DegC, the temperature profile might be divided in two zones. The first zone goes from 0 to 15 cm, while the second goes from 15 to 60 cm. The behaviour of the temperature in these regions can be approximated as linear and second order polynomial, respectively.

It is very important outline that the maximum temperature in the system is not reached at the outlet of the reactor, but it is located 10 cm before it. Temperature drops are observed for both Temperatures 350 and 600 DegC, but apparently, the higher is the furnace temperature, the more important the temperature drop is in the last 10 cm of the reactor. These temperature losses might be caused for the air flows ascending and escaping from the furnace. If fact, it was found that the use of an external insulation layer at the bottom of the furnace restricts the flow of ascending air inside the reactor. This ascending air currents not only generated a negative effect in the temperature of the water leaving the rector, but also in the temperature of the first zone of the furnace. Measurements of temperatures in the first zone of the furnace suggested that when using the insulation layer, a temperature increase of at least 30% was obtained.

Taking into account the findings of the low flow experiments, the temperature profile experiments at high flows were carried out after allowing a 6 hours time for thermal stabilization of the system. Results are summarized in the Figures 2.12 to 2.15.
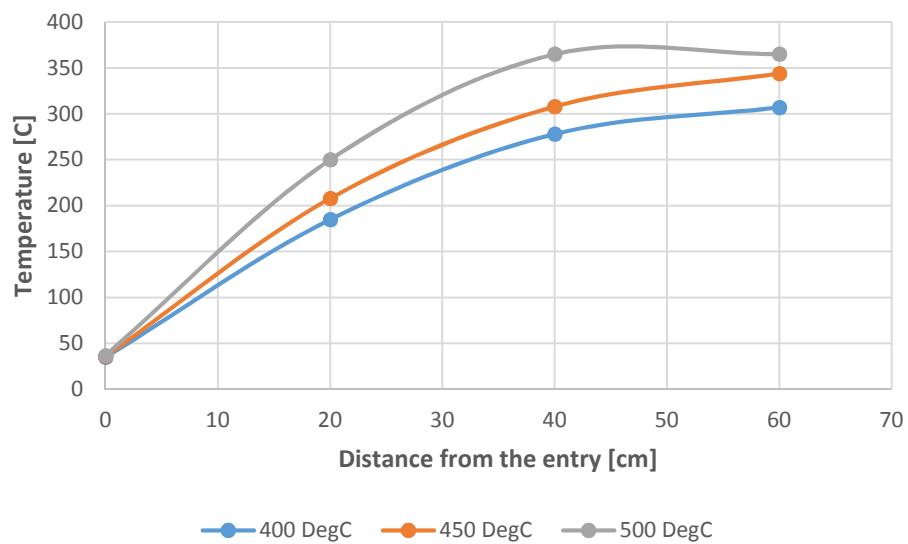
Figure 2.14. Water Temperature along the Reactor at different Furnace Temperatures @ 5 mL/min
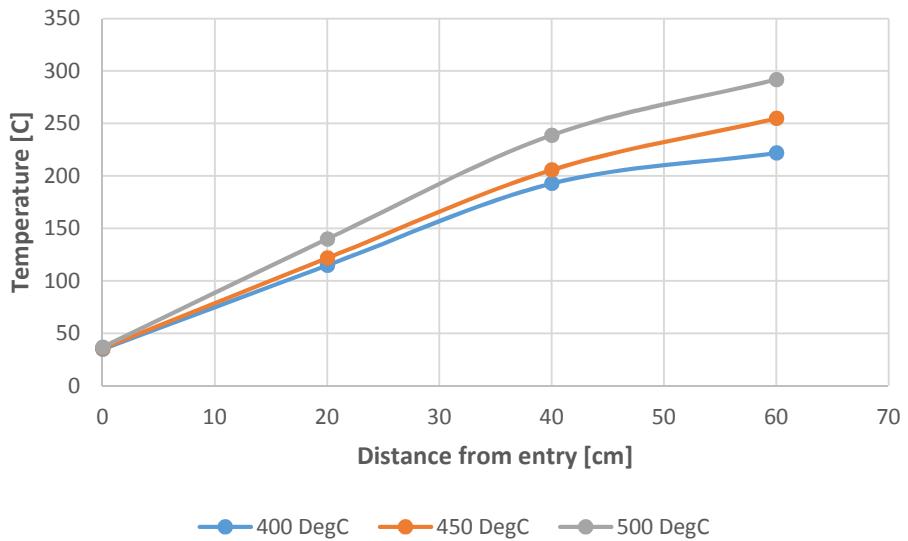
Figure 2.15. Water Temperature along the Reactor at different Furnace Temperatures @ 10 mL/min
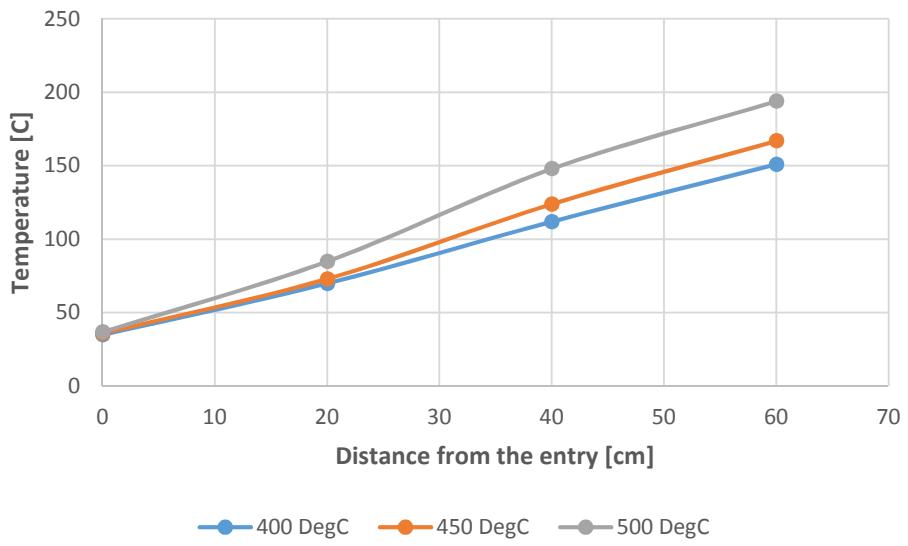
Figure 2.16. Water Temperature along the Reactor at different Furnace Temperatures @ 20 mL/min
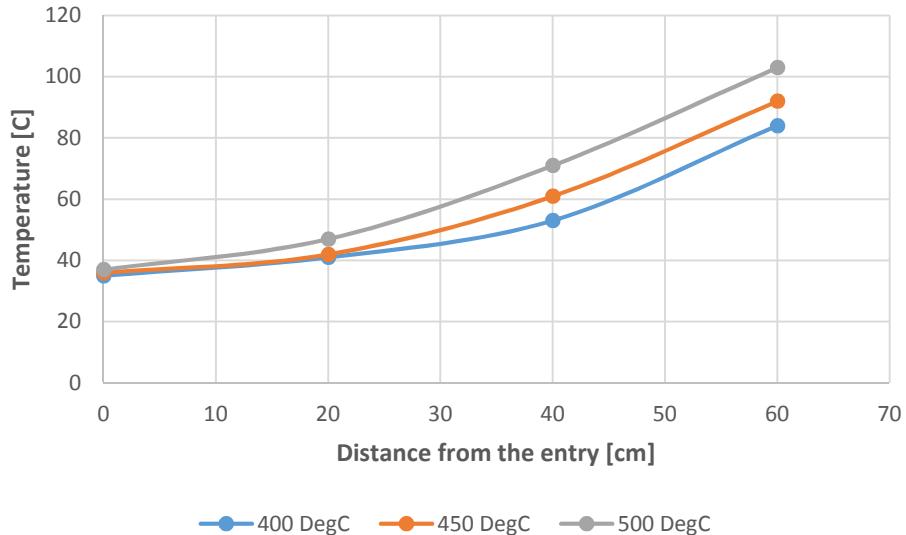
Figure 2.17. Water Temperature along the Reactor at different Furnace Temperatures @ 55 mL/min

2.2.3.3. Experimental Observations

It was observed that regardless the temperature, the flow rate heavily impacted the heating period of the system in two very different ways. At small flow rates, the furnace temperature stabilization was short, but the time required for the system to reach its steady state was very long. In the opposite manner, at large flow rates, large furnace temperature stabilized relatively slow, but the total system reached stabilization quickly, just a couple of hours. For instance, while for flow rates of 5 mL/min, a furnace heating time of nearly 20 mins and settling period of at least 7 hours was required, for 80 mL/min this time spaces were 45 mins and 3 hours.

Regarding to the stabilization time required when the flow rates were changed in a run, it was observed that they were proportional to the flow rate of water that was injected in that moment. For instance, when the flow rate was initially changed from 5 to 10 mL/min, a stabilization time of almost 50 mins was required. In the other hand, for 80 mL/min, just 15 mins were sufficient.

Preheating of the system was also tried under conditions of no flow. This implied that the system was firstly pressurized with Nitrogen and heated to stable state before any water injection. This methodology was not effective because when the water injection

was performed, the steady state condition was lost and large variations in the temperatures were observed. After occurrence of such variations, the system had to be leaved for and additional time for re-stabilization of the thermal steady state. In overall, the system consumed 2 hours more for total stabilization when compared with the other method. This experiment was carried out at a flow rate of 5 mL/min and at a furnace Temperature of 300 DegC.

Another important observation is with regards to the need of the initial pressurization. Despite the fact that system can be first flushed with water at atmospheric pressure, and afterwards pressurized by tightening the BPR; the valve showed a better pressure control in gas media than in liquid one. Also, it was observed that gas presence in the system contributed to a smoother pressure control (easily attributed to the compressibility of the gas). An example of this compressibility favourability to the pressure regulation was observed when comparing the pressure variations in both cases. In one hand, pressure variations of up 20-50 psi were observed when the system was not initially pressurized. In the other hand, this variations decreased to 6-10 psi when pressurization with Nitrogen was initially performed. It was also noticeable that pressure variations are most severe at higher flow rates than at low ones.

2.2.4. Reactor Enhanced Model

After concluding the experimental study of the reactor, it is clear that the proposed model in the section of modelling did not match with the reality. In fact, taking into account the results of the temperature profile experiments, it is obvious that the hypothesis of isothermal walls was not correct.

The fact of having no isothermal conditions in the reactor opened the question about the accuracy of the temperature measurement system and its suitability for these experiments. Some experiments at hot-open furnace conditions revealed that the thermocouples inserted through the furnace walls were not measuring the temperature of the surface of the reactor, but, instead, they were measuring the temperature of the hottest point in the ceramic walls of the furnace. This finding was supported by one experiment were an additional thermocouple was inserted from the

bottom of the furnace and it was fixed up to the mid-point, exactly where the central thermocouple inserted thought the walls of the reactor laid over the surface of the reactor. For the following conditions: Furnace Temperature of 450 Degrees, Flow rate of 10 mL/min, and a Pressure of 200 Bar, it was found that the reading in the thermocouple inserted through the walls of the furnace was 450 DegC, while the reading of the new thermocouple was 182 DegC. It is interesting to see, in fact, that the reading of the second thermocouple is closed to the reading obtained in the temperature profile for high flow rates in the previous section.

It was decided to make an additional experiment to properly assess the temperature profile in the outlet of the reactor. For this, three thermocouples were inserted from the bottom of the furnace, and fixed to the points were the original furnace thermocouples were in contact with the reactor's walls, as in Figure 2.2. The experiment was carried out at 1 and 2 mL/min conditions for 350 DegC set point in the furnace. The results of this experiments are summarized in the Table 2.6.

1mL/min 350 DegC		2 mL/min - 350 DegC	
Treact	**DegC**	**Treact**	**DegC**
Top	339	Top	334
Medium	300	Medium	284
Bottom	176	Bottom	165

Table 2.6. Reactor's wall Temperature for 1&2 mL/min

The previous results suggest that a correct model of the reactor has to include the isothermal ceramic walls of the reactor as well as the air space that exist between these and the reactor. Following the geometry described in Figure 2.2, a new Model for the furnace, including also a space of 2 mm between the reactor and the top and bottom surfaces of the reactor was developed in Comsol. The aim of the mentioned spaced was included the effects that the air currents entering and leaving the reactor may have on the temperature profile.

The New model included the effects of heat transfer by radiation from the furnace walls to the reactor's surface, as well as the effect of the natural convection caused by the

buoyancy effect in the air gap inside the reactor. The model was developed as a 2D isometric model and the modelled conditions were: Furnace temperature of 350 DegC and Pressure of 200 Bar. Figure 16 shows both: the thermal distribution inside the furnace (rendered from a 2D axis-symmetrical model), and the velocity field in the top part or the furnace, for a flow rate of 2mL/min.

From the results of this model it is possible to observe that there exist a boundary layer in the outer surface of the reactor that is at lower temperature than the temperature at the walls of the furnace. Such boundary layer is caused by the air raising for the bottom to the top of the reactor, caused mainly for the buoyancy effect, as it was already mentioned. The model also provides the reason for the abrupt temperature decrease at the outlet of the furnace. As it can be seen from the right hand side image of the Figure 2.18, the maximum air velocity reaches a maximum in the top passage of the reactor. This air at high velocities is translated into an increase heat transfer from the walls of the reactor to the air escaping the furnace.
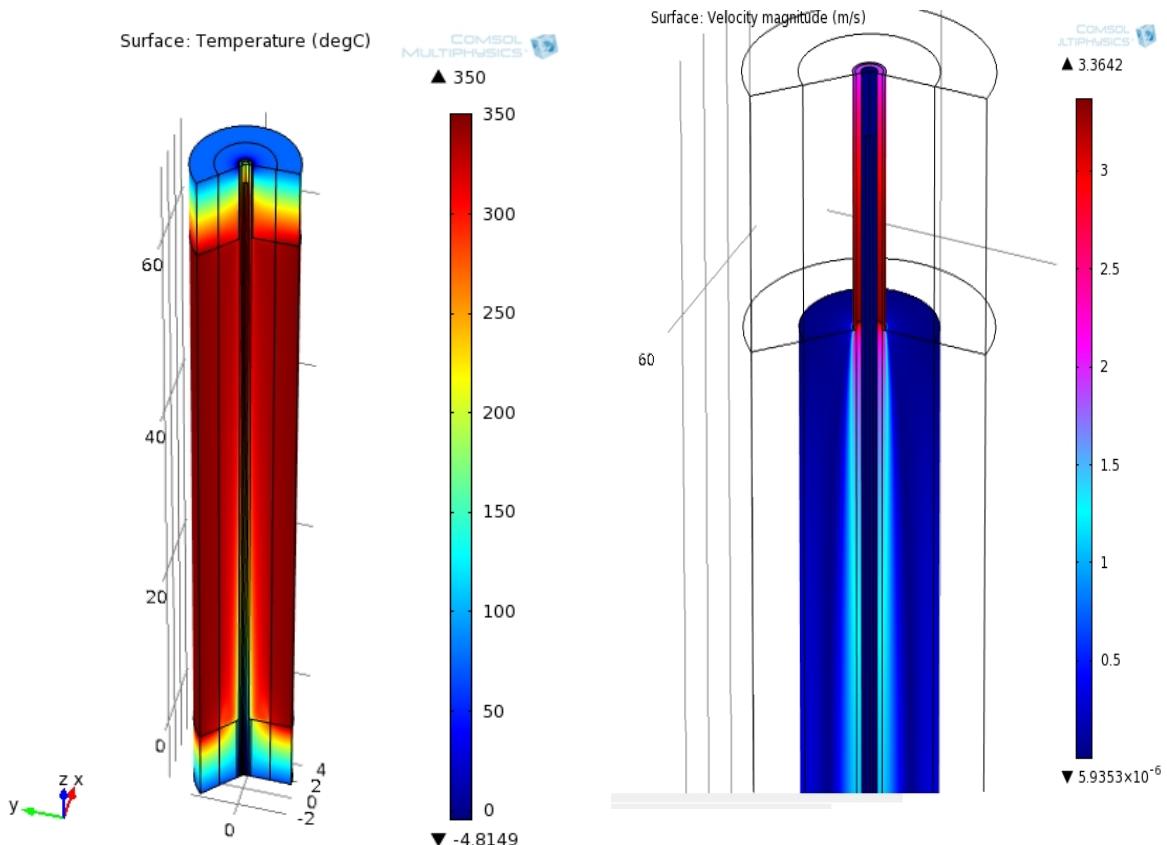
Figure 2.18. Left: Furnace Temperature. Right: velocity Fields inside the Furnace.

Figure 2.19 compares the temperature profiles obtained experimentally and by CFD simulation. The results shown that the CFD predicts the general tendency of the profile nicely, but a maximum error of nearly 25 degrees Celsius is observed at 45 cm. It can be said, however, that the model over predicts the thermal losses at the outlet of the reactor. This can be explained by the fact that the model allows the ascending air currents to leave from the furnace while in the reality, some additional insulation is been put at the top of the furnace. Despite this insulation does not block completely the air flux, it diminishes its velocity, therefore, decreasing also the thermal loses.
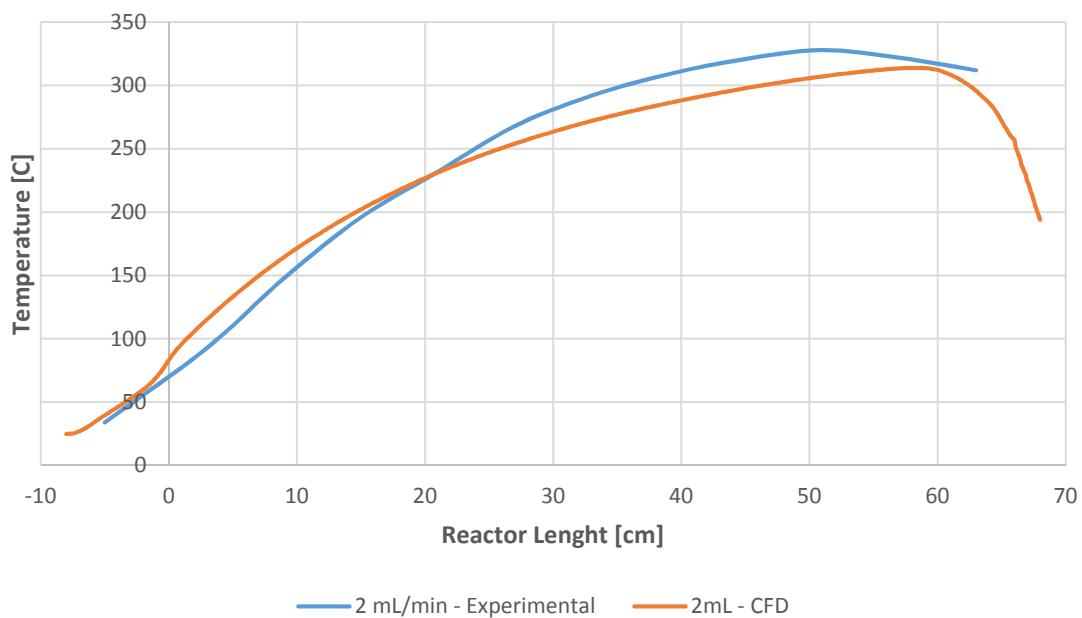
Figure 2.19. CFD vs Experimental temperature profiles.

2.3. Development of a New Liquefaction System

The experiments and the modelling tasks revealed big limitations in the overall heat transfer coefficient of the furnace. The inability of the furnace to increase rapidly the temperature of the water flowing through the reactor make that even at extremely low flow rates, 1 or 2 mL/min, only 20 cm of length where available for biomass placement. In addition, the furnace showed not to have a stable temperature profile along the

reactor, which in turn make impossible the study of liquefaction experiments at stable temperatures. Finally, the very long heating periods are completely unacceptable, because it is very likely that after 2 hours, when the system has not reached its steady state, all the biomass has already reacted.

2.3.1. First generation system.

The first thing that came in mind was the need of developing a new reactor out of the furnace, where the biomass can be placed and keep at low temperatures at the same time while the system reaches its steady state. Based on the traditional Set-up of continuous liquefaction systems, as depicted in Figure 3, it was thought to use the Parr reactor only as a preheater device where the water is brought to a subcritical state, followed by a new reactor equipped with a by-pass line. In addition, this topology presents a huge advantage in terms of a very high heating rate, as long as the water entering the reactor is already at the reaction temperature and no time for heating the reaction media is required. The schematic of this system is given in Figure 2.20.
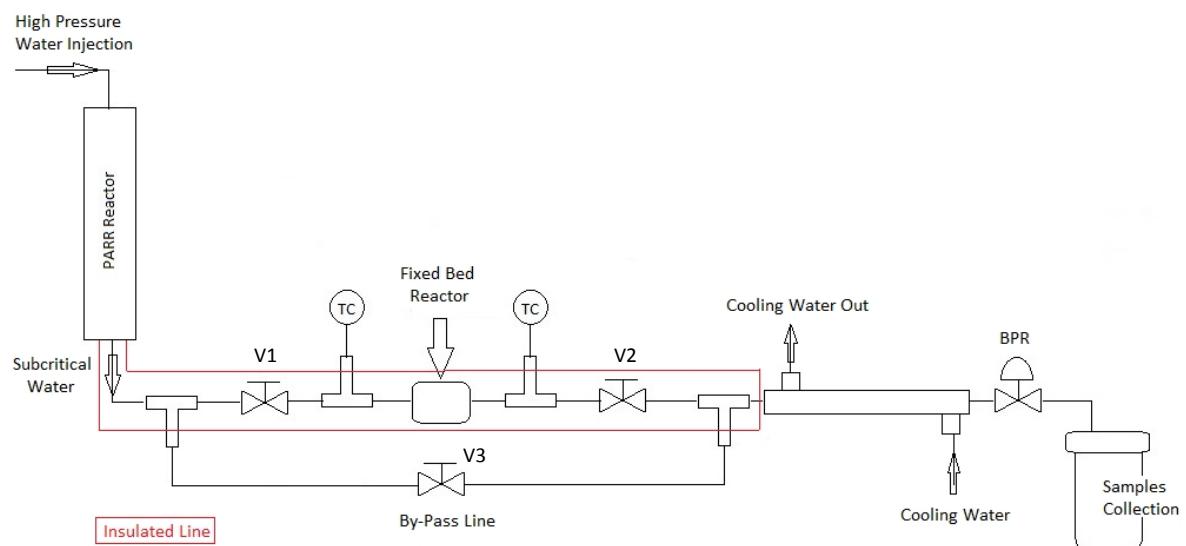
Figure 2.20. New Liquefaction System

The philosophy and the operating conditions of the proposed topology are summarized as follows:

1. The system is initially pressurized with valves V2 and V3 opened, and V1 closed.
2. Water injection is performed until the point where the whole system is full of water.
3. The furnace is turned on while pumping is performed and thermal stabilization is allowed.
4. After thermal stabilization, V3 is closed and V1 is opened, simultaneously.

The design of the Fixed Bed Reactor was reduced to one single requirement: its capacity to hold at least 3 grams of Biomass. This amount of mass was selected to be our reference in order to compare the obtained results here with the obtained ones by Hashaikeh et al, in his study [30]. In fact, very few studies have studied the liquefaction process in fixed bed reactors. [30][31][32].

2.3.1.1. R&D Process

The development of the new system implied many challenges, but the biggest one was to build up a reactor that:

- Withstand conditions of high temperatures and pressures.
- Offers easy opening, closing and cleaning procedures.
- It is able to hold at least 3 g of biomass.
- It is easy and cheap to build up.

Most of the reactors that satisfy the previous conditions are made up of one piece of metal and have one lid for easy opening, one example of this type of reactor is the collection vessel of the 5104 system. Despite the thermal lab has the possibility of machining a single metal piece to convert it into a reactor, for safety regulations, it is not allow to use homemade reactors over pressures of 20 Bar. Due to this restriction, the only possible solution for a new reactor was to use standard fittings and tubes to build the new reactor. Following this idea, two reducers, two male connectors and a straight coupling were used as reactor.
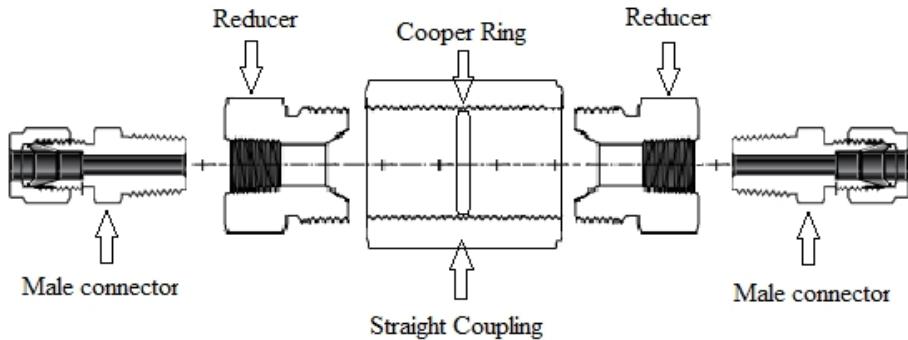
(a)

(b)

Figure 2.21. (a) Schematic of the Reactor. (b) Reactor with graphite sealing.

The reactor as showed in the Figure 2.21 offered a total internal volume able to hold up to 2.5 grams of biomass in chips of 2 mm, but unluckily, in the first pressure test, leakage was present at pressures over 35 bar. The leakage was avoided by the introduction of a cooper ring in the interior or the reactor. The cooper ring was the selected solution after having performed a series of experiments where rings made up Teflon and graphite where tested. In those experiments, Teflon shown to withstand up to pressure of 200 Bar but its drawback was its low melting point of 265 DegC. The graphite ring, in the other hand, was suitable for temperatures over 500 DegC but its

sealing performance was not good. In fact, leakage was detected for the graphite ring at pressures over 60 bar.

The development of the new liquefaction system involved the ordering of new pieces such as proper fittings and valves for the system. For instance, valves were another important element in the system, as long as they must be able to work in conditions of up to 200 Bar and 350 DegC. The only set of valves in the market able to withstand such conditions were the SS-3NRS4-G from Swagelok. These valves, normally used in the oil industry, were available only at a tubing diameter of 1/4 inch. Therefore, this dimension was selected as the standard for tubing of the whole system.

The next step in building the system was to find a suitable position for the new elements in the bench of the Parr System. In the first attempt, the reactor branch was placed horizontally in the place where the second gas inlet line was initially located. With this design, it was possible to support properly the new tubing line to the frame of the bench, avoiding at the same time the relocation of the BRP to a new location. The thermal insulator used around the line connecting the outlet of the Parr Reactor and the new system was GLAVA LAMELLMATTE fiberglass, material normally used for thermal insulation of ducts. The Figure 2.22 shows the result of this first attempt.
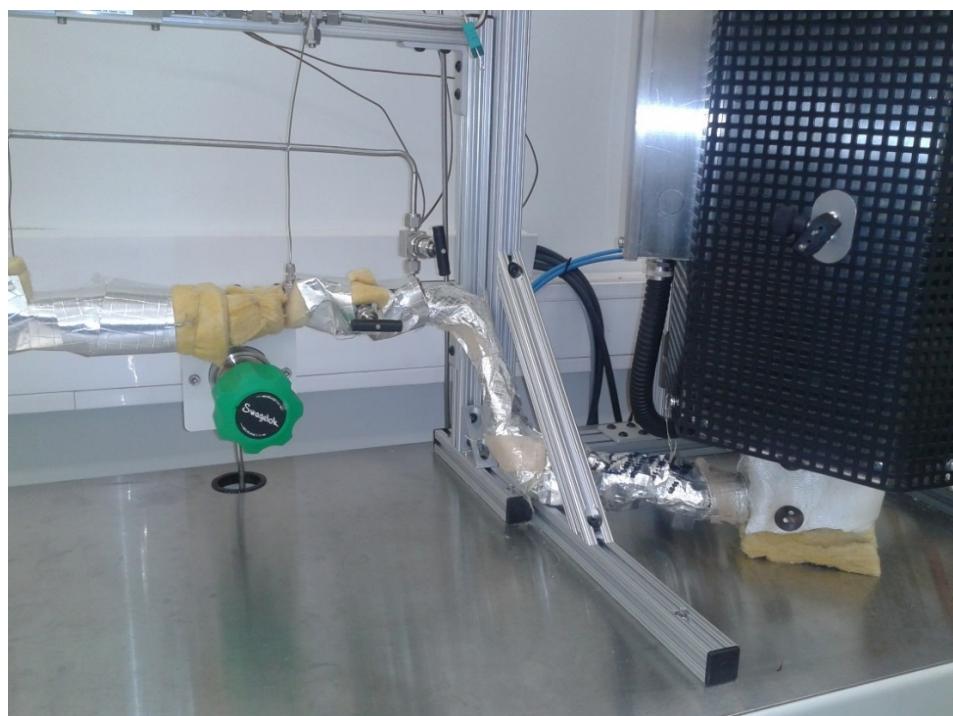
Figure 2.22. First Insulation attempts

After having assembled the system, a performance test of the new configuration was carried out for the following experiment conditions: 100 bar of pressure, furnace temperature of 550 DegC, and water flow rate of 5 mL/min. This experiment revealed huge heat losses problems in the piping connecting the Parr Reactor and the Fixed bed Reactor. In fact, for this operative conditions, the subcritical water flowing through the tubing decreased its temperature by 140 DegC in the 47 cm of tubing. After additional experiments with this configuration, it was noticed that most of the heat losses can be notably decreased by increasing the flow rate of the fluid. Increments in flow rate can be translated as shorter residence times, therefore, lower heat losses. Furthermore, it was noted that in the closer part to the Parr reactor the insulation was dramatically burnt. In addition to all above, it was also discovered that shortening the by-pass line as much as possible, and its further insulation helped to decrease the heat losses.

Based on the previous observations, it was decided to move the new reactor branch to the lower part of bench, immediately after the Parr reactor, then reducing the length of the connecting tubing to only 12 cm. The relocation of the fixed bed reactor to the bottom of the bench also forced to re-designing the system, as long as the available space in this part of the bench was much smaller than in the top. Reduction in volume of the system was also an advantageous thing from the thermal point of view, because the smaller the system is, the smaller is the area of heat transfer between the system and the environment.

In order to reduce the space required for the system, some configurations based on square arrangements instead of the basic rectangular one were tested. After some weeks of R&D, the developed system was able to reach a temperature of 280 DegC at the inlet of the reactor for conditions of 150 bars of pressure, 600 DegC furnace temperature, and water flow rate of 15 mL/min. Table 2.8 summarize the operative conditions and the temperature readings.

System Generation	Flow Rate [mL/min]	Pressure [bar]	Furnace Temperature [C]	Parr Outlet Temperature [C]	Fixed bed reactor Temperature [C]
1	15	150	600	320	285

Table 2.7. Performance of the First Generation system.

Among the main modifications performed over the system, one can count:

- The replacement of the GLAVA LAMELLMATTE insulation for a new insulation system based on a thick layer of 6 cm Rockwoll insulation.
- The introduction of a feeding line located at the outlet of the fixed bed reactor, needed guarantee the total filling of the system with water.
- Replacement of 1/4" for 1/8" tubing in the by-pass line.
- Addition of a thermocouple in the by-pass line in order to confirm steady state condition before performing the opening of the valves.

Figure 2.23 shows diverse stages on the evolution of the system.
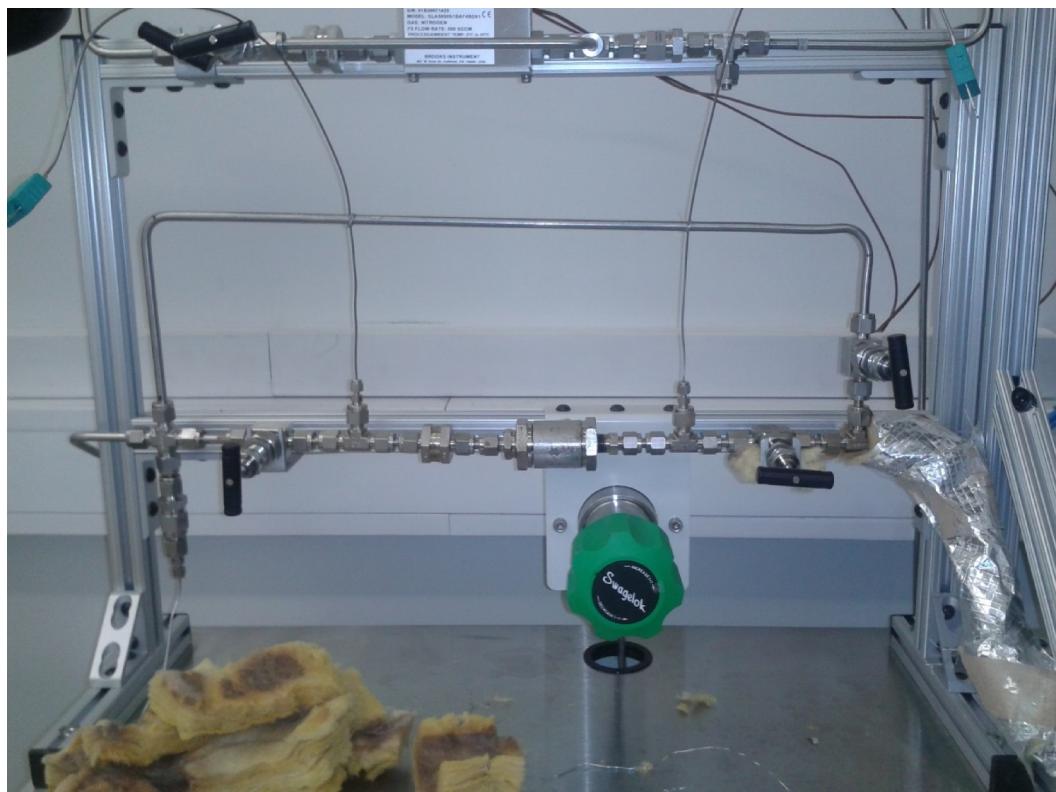
(a)

(b)

(c)

(d)

(e)

Figure 2.23. Evolution of the system. (a) First Rectangular configuration on top of the bench. (b) Overview of the system with the reactor branch in the bottom of the bench. (c) Squared arrangement of reactor and By-pass line. (d) Amorphous arrangement tested to reduce as much space as possible. (e) Issues with the insulation of the configuration (d).

2.3.1.2. First Biomass Experiments.

After having completed the modifications to the system, 1.5 grams of 90 um Norwegian Spruce sawdust biomass dried overnight at 105 DegC, were loaded to the reactor and a liquefaction performance test was run. Norwegian Spruce was characterized by Bertaud ed all [33] and its composition is given in Table 2.8. The planned experiment conditions were 280 DegC in the fixed bed reactor, 150 bar of pressure, 15 mL/min of flow rate, and a reaction time of 45 mins.

Biomass Composition	Percentage [%]
Cellulose	45
Hemicellulose	25
Lignin	35

Table 2.8. Norwegian Spruce Composition

The experiment was carried out following the described philosophy in the previous section, but only after 2 minutes of experimentation (after 2 minutes of having opened V1), a leakage in the reactor took place and huge amounts of vapour of sweet smell were scaping out from the system. After stopping the experiment, the system was inspected and it was noticed that small particles of biomass were attached to the cooper ring, preventing proper sealing of the reactor. This issue was dramatic for the system because it was noticed that the only possible solution to overcome the problem was to load the reactor up to only half of its capacity.

In addition to the leakage in the cooper ring, it was also noticed that some vapours were scaping out from the reactor in the point where the male union is screwed in the ball union. Having into account that it was not possible to find cooper rings of a suitable dimension for this union, it was decided to weld the two pieces as is shown in Figure 2.24. The welded reactor was tested up to pressures of 250 bar and no leakage was present.

Figure 2.24 Welded Reactor

After reloading the welded reactor with only 0.7 gram of new fresh spruce, the experiment was run again without inconvenient. After concluding the experiment, the reactor was took out from the system and cleaned with fresh distilled water and acetone. The solid particles where collected via filtration with a paper filter and dried overnight at 105 DegC. After drying, the samples were weighted in an electronic balance of resolution of 0.1 mg, and the liquefaction efficiency or conversion efficiency (3), was calculated.

$$Eff = \frac{m_i - m_f}{m_i} * 100\% \qquad (3)$$

Where:

m_i: Initial biomass loaded into the reactor [gm]

m_f: Remaining biomass in the reactor [gm]

The obtained conversion efficiency for the experiment was 64.7%. This is a coherent value because at 280 DegC, total decomposition of hemicellulose and lignin was expected. Furthermore, it can be deduced that some of the cellulose of not crystalline nature underwent into dissolution as well. This phenomena has been previously reported [30].

2.3.2. Second generation system.

The unexpected issues when loading the reactor that reduced its effective capacity to half of the total one, made the developed reactor not appropriate for further study of the liquefaction process. In the second generation system, not only a new reactor was designed, but also some modifications and enhancements were done to the system.

2.3.2.1. R&D Process

From the previous experience, it was clear that to avoid any problem when filling up the new reactor, it should be made of a single piece with no threads in the interior in order to make easier the cleaning process. Two reactors were built out of SS 316 tubes of 1" and ½" and standard Swagelok fittings. The length of each reactor was calculated to obtained internal volumes of 30 and 15 mL for the 1" and ½" respectively. In theory, one of the ending fittings should work as lid for the reactor, and it should be opened and closed for loading and cleaning procedures. The use of these new larger reactors allowed also the introduction of a thermocouple inside the reactor, therefore improving the measurement of the liquefaction temperature. This modification also contributed to the reduction of space, as it allowed to take out from the system the T connection used at the outlet of the reactor for temperature measurement.
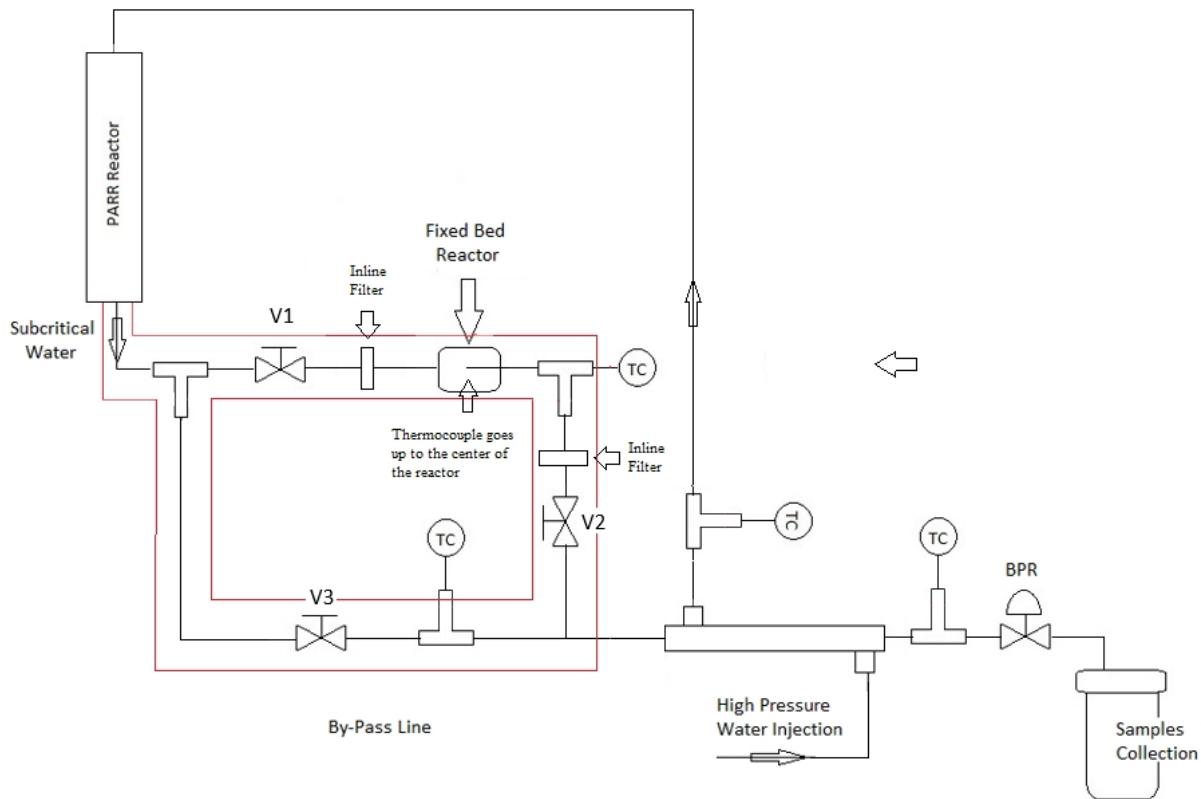
Figure 2.25. The Second Generation System.

In order to increase the maximum dissolution temperature that the system was able to reach, a configuration in which the cooling jacket was used as economizer was adopted. In this new Set-up, the jacked was used as a counter-current heat exchanger in which water was first pre-heating, and afterwards sent to the Parr Reactor.

The introduction of In-line filters immediately after and before the reactor was a practical enhancement to avoid dispersion of biomass through the whole system, as well as they will help to collect particles when cleaning the system.

2.3.2.2. Development of a PC application for Temperatures measurement.

The temperature readings in the first generation system was done by connecting the thermocouples to a two portable thermocouples readers that were borrowed from NTNU's Thermal Lab. However, the addition of new temperature measuring points to the system created the need of changing the way in which temperatures were being

controlled. In this sense, the second generation system was enhanced with a 4-chanels thermocouple input device from National Instruments.

The use of the A/D Thermocouple reader was originally received with a LabView application that had to be reprogramed because it was been developed for measuring temperatures in only two out of the four channels in device. The LabView re-programming tasks included the addition of the required blocks for properly set-up of the logging life, reading and visualization of the new channels, and the reconfiguration of the DAQ Assistant block. A screen shot of the Lab view application is shown in the Figure 2.26, where the temperature readings are displayed in DegC. Figure 2.27, instead, shows the block diagram of the application.

Calibration of the temperature readings was initially performed for each channel having a FLUKE 725 Process Calibrator as pattern device (Calibration date: 07-03-2013). Calibration was made for the range of 5 to 600 DegC, taking readings at 5, 50, 100, 200, 300, 400, 500 and 600 DegC.

Another advantage of the LabView application was the possibility of recording the temperature readings of the four channels for further analysis and plot. The application stores the data in a TXT File that can be easily imported from Microsoft Excel.
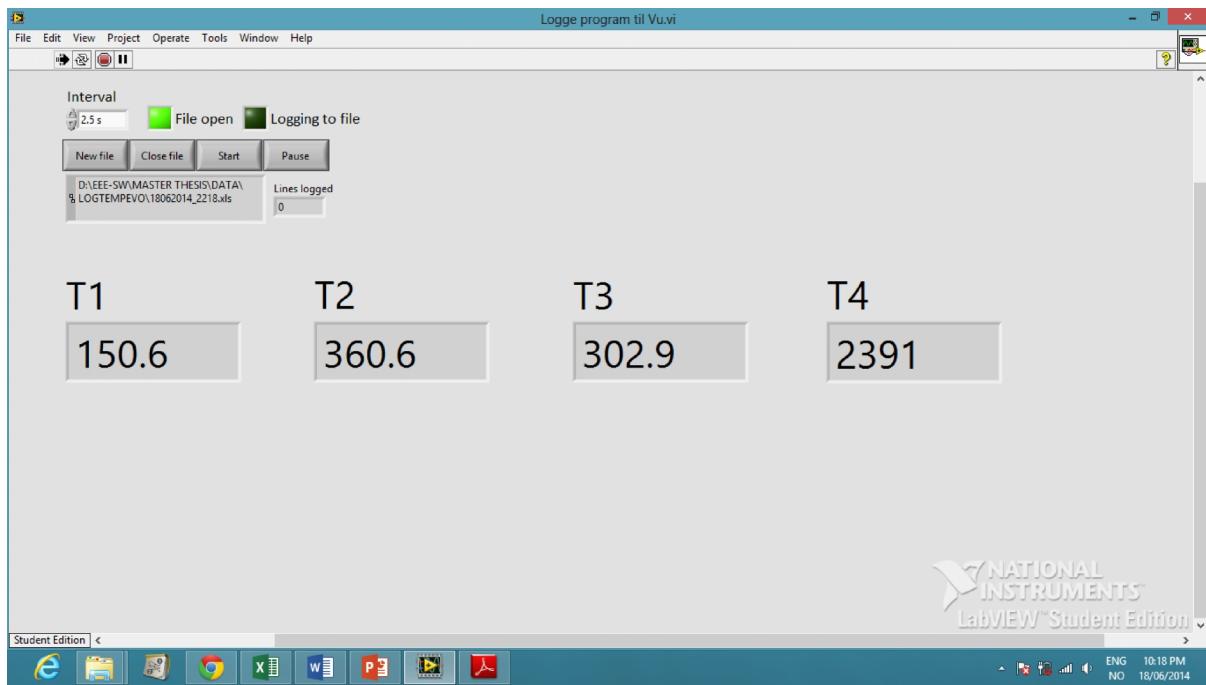
Figure 2.26. Lab View Temperature Logging Program Front Panel.
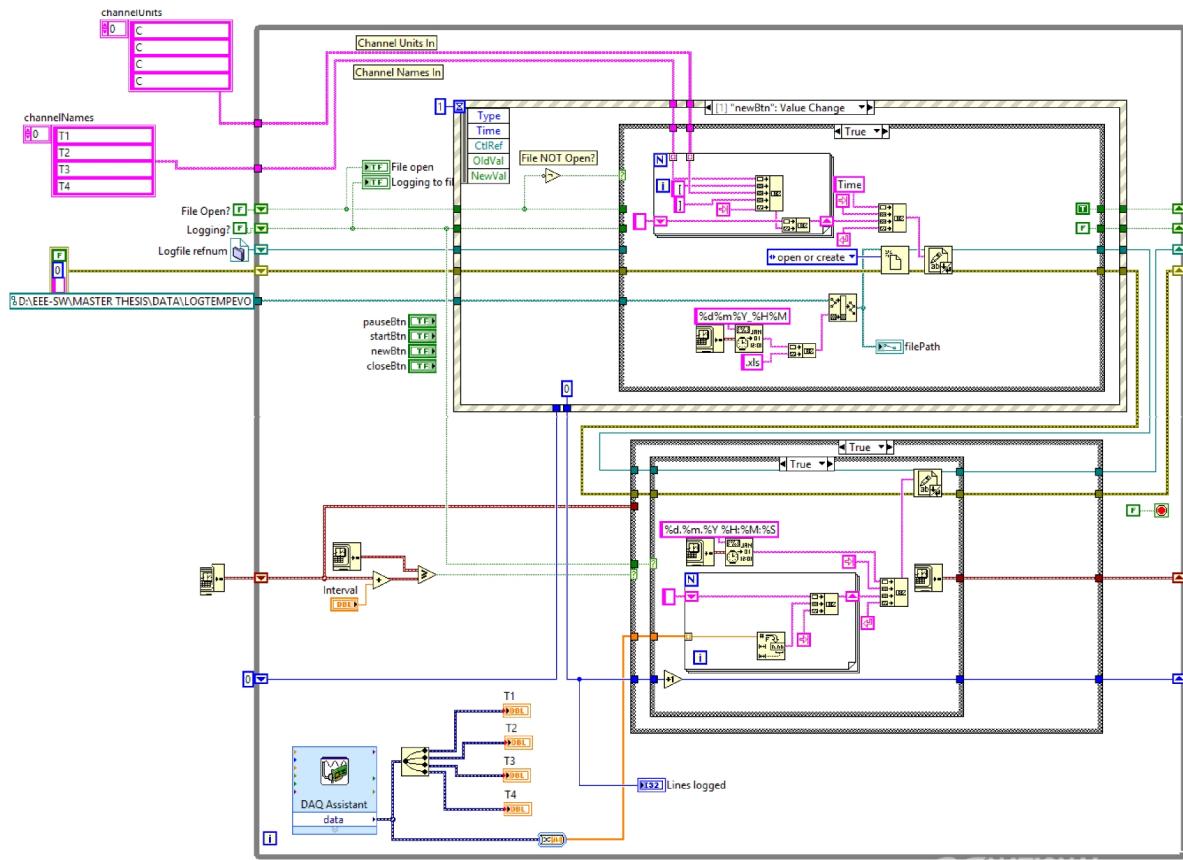
Figure 2.27. Block Diagram of the program.

2.3.2.3. The issues of the second generation system

2.3.2.3.1. Reactor Selection

A test pressure and performance tests for both reactors: 1" and ½" were carried out flowing to the described methodology in the section 2.1.3 for pressurization, water injection and temperature testing of the system. In general, the system showed a good performance up to pressures of 200 bar. Over this pressure level some leakage was observed in the valve V1, when it remained at closed state.

A performance test was run for both reactors at conditions of 150 bar of pressure, Furnace Temperature of 600 DegC and flow rate of 15 mL/min. The first difference noticed between the use of one or another reactor was the time required for the thermal stabilization of the system, being these times of approximately 6 hours for the small reactor and 7 hours for the large one. However, the biggest difference between one and another reactor was the time required for bringing the temperature inside the fixed bed reactor from its initial state to the one at which the liquefaction would be carried out. In this context, it is called initial state to the condition at which fixed bed reactor is after the 6 or 7 hours required for thermal stabilization, just before opening V1 and closing V2. In fact, the heating times for the small and big reactors were nearly 10 and 45 minutes respectively. At this point it was knew that the heating time of the big reactor was unacceptable and that it must be improved. In fact, some modifications, as the addition of a preheating line rapped around the external surface or the reactor were carried, but no major improvements were obtained. Figure 2.28 shows the new installed heating line around the reactor.

Figure 2.28. Big Reactor and Additional heating line.

After the previous experiments it was concluded that for water flow rates and temperatures in the order or 20 mL/min and 300 DegC respectively, the big reactor cannot be used due to its huge thermal inertia. In fact, as the big reactor is able to store more than 4 times the water that the small one can, it is reasonable that the heating time of the big reactor is almost 4 times larger than the small one. This effect is mainly explained by the fact of the predominance of the heat capacity of the water over the one of the SS 316. This hypothesis is partially confirmed by the calculation of the energy required to increase in 300 DegC the temperature system:

$$Q = (mc_p\Delta T)_{Reactor} + (mc_p\Delta T)_{Water} \qquad (4)$$

Reactor	Weight [gm]	Capacity [mL]	Energy required to raise 300 DegC [KJ]
First gen Reactor	350	8	62.3
1″ Diameter (Big Reactor)	767	50	176.8
½″ Diameter (Small Reactor)	283	12	57.3

Table 2.9. Reactors Characteristics

According to the results obtained, the big reactor requires 3.08 times as much energy as the one that the small reactor requires to increase in 300 DegC the temperature of the system. It is important to mention that the previous energy calculation was made under the assumptions of no flow conditions and to thermal losses. However, the previous calculation is helpful in giving and idea of the energy consumptions of the system in the heating up period (before reaching steady state). It is also interesting to see that the ½" Reactor is much more energy efficient than the one used in the first generation system. To summarize the discussion above given, it is concluded that the ½" rector is the most suitable for the liquefaction experiments at the studied flow rate conditions, therefore, this reactor is selected for the second, third and fourth generation systems.

Finally, it is very important to mention that these reactor characterizations were performed without the heat recovery scheme, because as it will me mentioned later, it will affect the preheating time of the reactor.

2.3.2.3.2. System performance tests

After the selection of the most suitable reactor, a performance test aimed of evaluating both the impact that the heat recovery had in the system and the heating time was carried out. In the experiment, the temperature at the outlet of the jacket, at the outlet of the Parr reactor and inside the liquefaction reactor were measured. The results of these experiments are summarized in Table 2.10.

System Generation	Flow Rate [mL/min]	Pressure [bar]	Furnace Temperature [C]	Temperature @ Jacket's outlet [C]	Temperature @ Parr Outlet [C]	Temperature @ Liquefaction reactor [C]
1	15	150	600	N/A	320	285
2	15	150	600	238	333	303
2	15	210	650	262	371	354
2	55	210	780	243	364	355

Table 2.10. Performance of the first and second generation system.

It is interesting to notice that despite a considerable temperature raise was obtained by the use of the heat exchanger, the temperature at which the water leaves the Parr reactor did increase only in 13 DegC if it is compared with the first generation system. This situation might be explained, in one hand, by the presence of huge thermal losses in the very long tubing required to connect the outlet of the cooling jacket with the inlet of the Parr Reactor. On the other hand, and perhaps more importantly, it is the problem with the very low heat transfer coefficient inside the furnace. In fact, the fact of having a temperature difference of 300 DegC between the walls of the furnace and the reactor wall, suggest that a major intervention has to be done in the furnace to improve its performance.

Although the modest increment in the temperature of the fluid leaving the Parr reactor in this second configuration, a valuable increment of 18 DegC in the dissolution reactor was obtained. Having into account that the increment between the outlet of the Parr reactor and the dissolution reactor was larger than the gain in temperature at the outlet of the Parr reactor itself, it is concluded that the new set up proved to be more efficient in both thermal losses and space occupied by the system.

Another issue of this second generation system was its stability. When the heat recovery scheme was implemented, it was noticed that small changes in the flow conditions induced large variations in temperatures. This effect of feed-back caused not only instabilities, but also larger temperature stabilization times, in fact, it was also observed that when the change of flux was performed (from by-pass line to reactor line), the outlet temperature at the jacket decreased, therefore decreasing the rest

temperatures in the system. The time required for the system to overcome this rough patch in the temperatures was nearly 30 minutes.

Figures 2.29 and 2.20 show the behaviours of the system with regards to its heating time for two different flow rates, 15 and 55 mL/min. As it was expected, the heating time of the system at 55 ml/min is shorter than the one at 15 mL/min. This is because the increase in the flow rate increments the energy entering into the system. If fact, the heating time at 15 mL/min is nearly 8.3 mins, while at 55 mL/min is 4.45 mins. In addition, this figures also revealed that the negative impact of the feed-back effect in the system increases with the increment of the flow rate. The larger the flow rate, the more intense and fast this phenomenon occurs.

Another issue that emerged from this experiments was that the initial temperature in the Liquefaction reactor, just before opening the valve V1, reached the value of 150 DegC. This temperature is excessively large, having into account that depolymerisation of hemicellulose can start at 180 DegC. This issue was solved in the third generation system by the introduction of a tubing raped around the reactor, this time not with the aim of preheat the system, but the aim of cooling it.
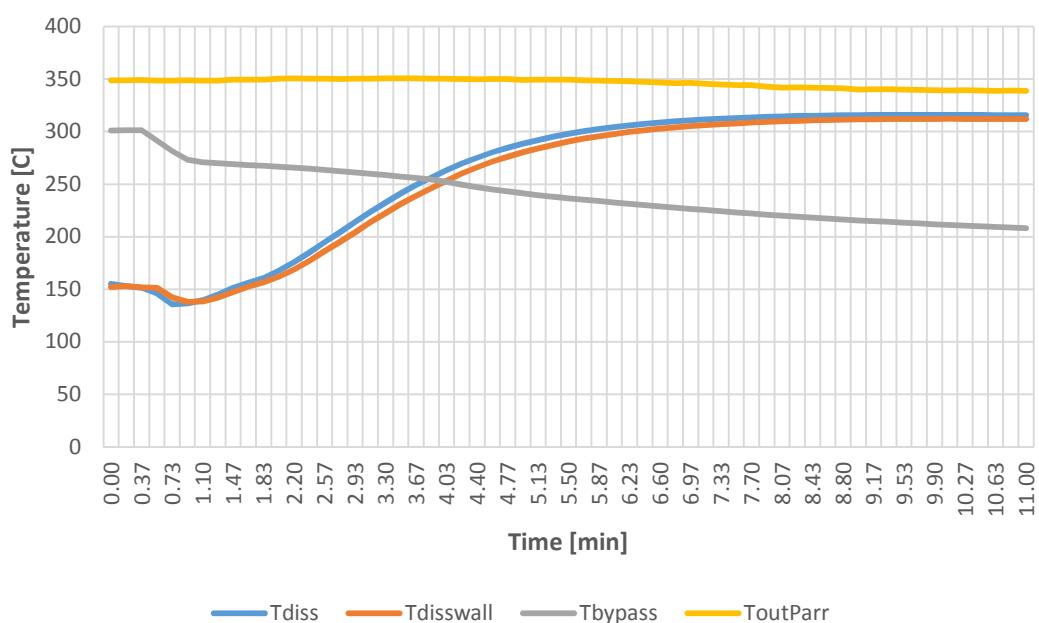
Figure 2.29. ½" Reactor Heating time @ 15 mL/min
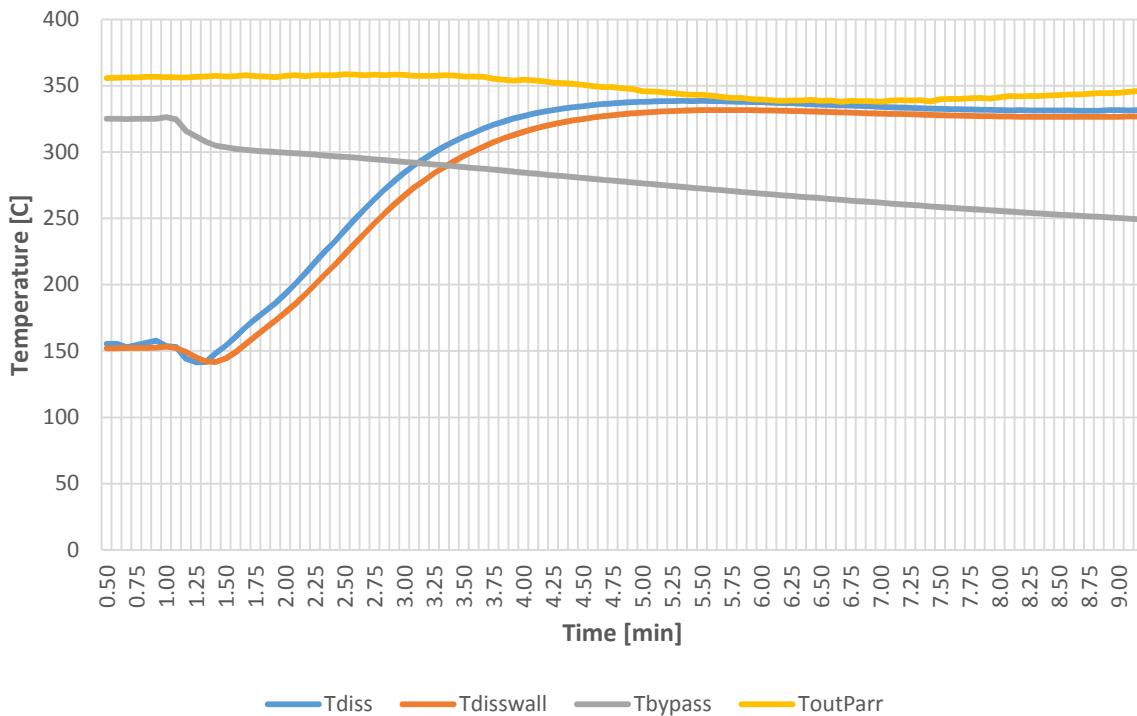
Figure 2.30. ½" Reactor Heating time @ 55 mL/min

2.3.3. Third generation system.

The third generation system was developed not only with the aim of overcoming the big problems that the system had especially with regards to the heat transfer phenomena inside the furnace, but also the whole set up was modified in order to improve its usability.

2.3.3.1. R&D Process

In the first place, it was decided to replace the Parr reactor inside the furnace for coil made up 1/8" SS 316. This diameter was selected from a trade-off process that included the following variables:

- Easy to bend
- Lower diameters improve the heat transfer from walls to liquid

- Larger diameters increment the residence time in the furnace, therefore incrementing the chance of higher temperature at the outlet of the furnace
- Larger diameters help to prevent any clogging or unexpected blocking in the tubbing.

The length of the tubbing was 18 meters total, and it was built out of 3 pieces of 8, 6 and 4 meters that were found in the thermal lab.

Regarding to the topology of the system, it was decided to eliminate the reheating configuration and to continue with the general scheme of the first generation system, as long as a huge improvement in the heat transfer inside the furnace was expected. Modification to insulation were also performed. In the previous generations, the rockwoll layer was raped around the parts and tighten to them by means of malleable still wires. However, this configuration carried major inconvenient as long as it wasn't been built thinking on the opening and closing usability that the insulation might have, for allowing the extraction the replacement of the reactor before every single experiment. In particular, it was observed that at temperatures over 250 DegC, the rockwoll sticked to the tubbing, making difficult its opening. These inconvenient were solved by rapping a high temperature fibber cloth around the rockwoll, in the interior and exterior parts, giving to the insulation system a better structure as well as adding an additional insulated layer.

Another of the major improvements in this system was the re-location of the dissolution reactor and its by-pass line from the bottom to the top of the bench. This modification help to highly improve the ergonomics of the system, as long as in the first and second generation system the operator of the reactor had the need of collecting the samples from a high of 20 cm from the floor, condition that forced the operator to sit in the ground. The re-location of the dissolution system implied that that reactor had to be fed from the bottom part, and not for the top, as it was in the previous cases. Feeding from bottom the system also implied that the line connecting the outlet of the furnace to the reactor should have a very thin diameter, in order to reduce as much as possible the heat transfer area and the residence time of the fluid, therefore reducing the heat losses in this part of the system. A tubbing of 1/16" was selected for this purpose.

Another interesting modification to the system was the change of the points were the gas feeding and the pressure measurement were done. For convenience, the gas feeding line (for initial pressurization), was moved from the inlet of the heating coil (previously Parr reactor), to a T point located just before the back pressure regulator. This modification also implied that the pressure measurement would be made not at the inlet of the system, but at the outlet. This change is particularly advantageous having into account that the Pre-pump has an additional pressure measurement device that allows to take control of the pressure at the inlet of the system. In conclusion, by measuring the pressure with the gauge at the outlet of the system, while in the inlet the control is directly made from the pre-pump, the system is enhanced with the possibility of identifying pressure losses and blockages.

Finally, the 40 mL/min pump was connected to the cooling jacket to circulate water as cooling fluid. Pumping was performed at maximum capacity of the pump.

2.3.1.2. Performance Tests

A new performance test was carried out following the methodology described in the section 2.2.3.1.1. However, not only the temperature at the outlet of the furnace was recorded, but most importantly, the effect of the temperature furnace over the temperature inside the dissolution reactor was studied for temperatures range from 200 to 400 DegC, and the flow rates of 20, 40 and 60 mL/min. The results of this study are summarized in the Tables 2.11 to 2.13. The results were also plotted in Figures 2.31 to 2.33, revealed a linear behaviour of the system.

TFUR	ToutParr	Tbypass	Tdiss
[C]	[C]	[C]	[C]
200	173	156	160
250	220	196	200
300	260	233	245
335	295	267	278

Table 2.11. System Characterization at 20 mL/min

TFUR [C]	ToutParr [C]	Tbypass [C]	Tdiss [C]
250	157	174	162
300	197	202	201
350	237	247	239
395	272	280	274

Table 2.12. System Characterization at 40 mL/min

TFUR [C]	ToutParr [C]	Tbypass [C]	Tdiss [C]
300	170	171	178
350	213	213	219
400	252	248	257
450	289	285	295

Table 2.13. System Characterization at 60 mL/min
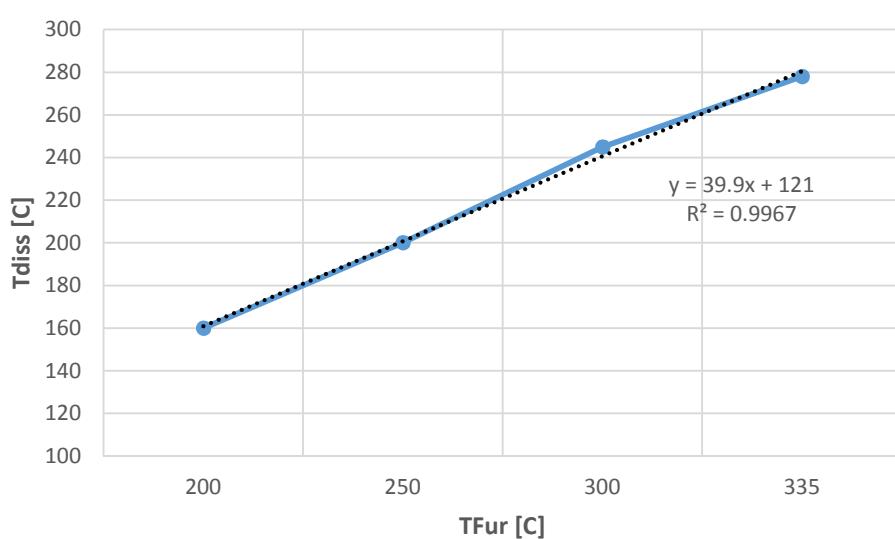
Figure 2.31. Temperature at the Dissolution Reactor vs Furnace Temperature at 20 mL/min
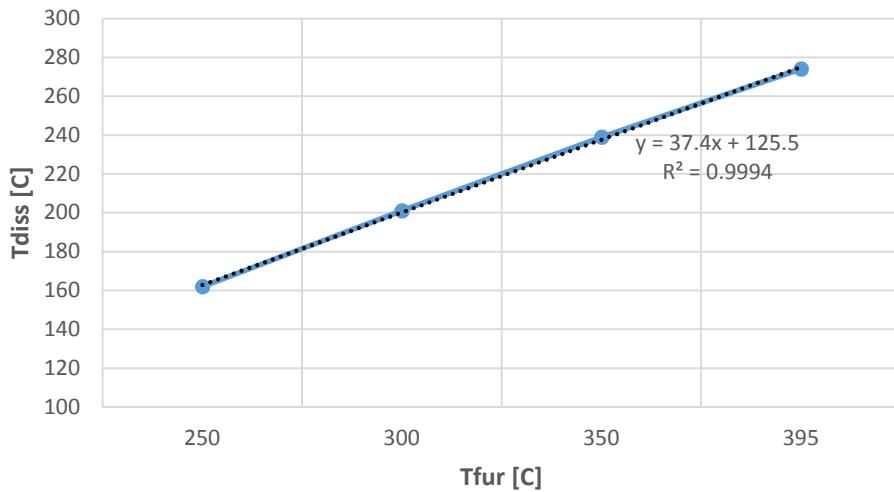
Figure 2.32. Temperature at the Dissolution Reactor vs Furnace Temperature at 40 mL/min
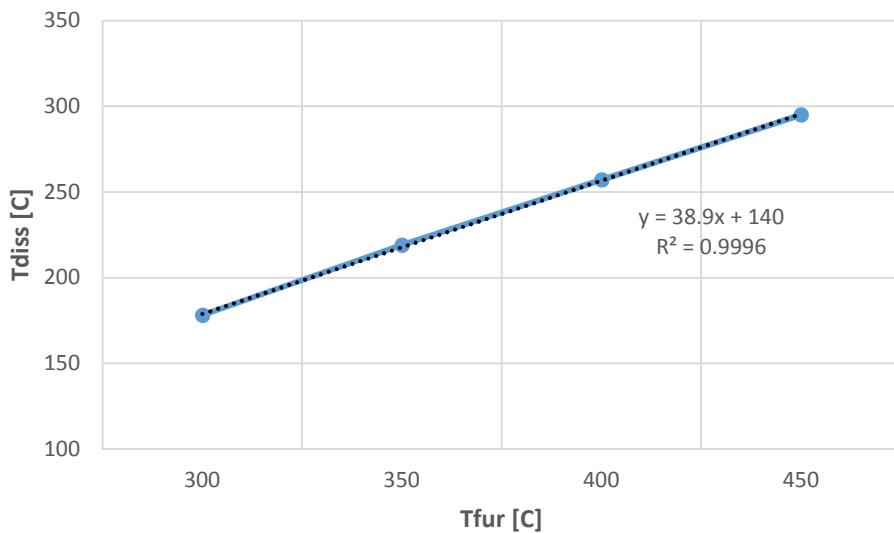
Figure 2.33. Temperature at the Dissolution Reactor vs Furnace Temperature at 60 mL/min

The results, as expected, showed that the new system has a much better performance in terms of heat transfer inside the furnace than those of the first and second generation systems. Moreover, another big advantage of this system is its faster thermal stabilization time, which has been reduced to only 1.5 Hours. Figure 2.33

shows the results of the heating time experiment for a flow rate of 20 mL/min at three different liquefaction temperatures: 175, 225 and 275 DegC.
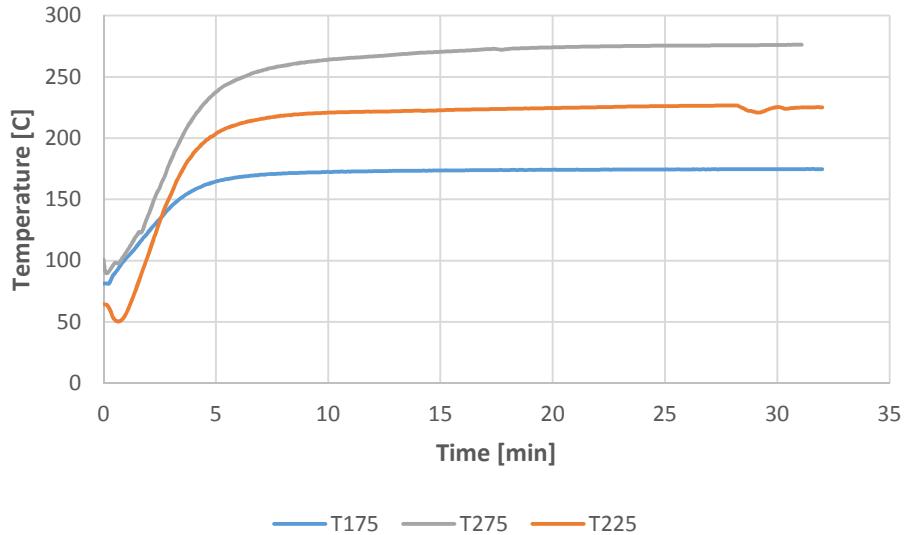
Figure 2.34. Reactor heating time at different liquefaction temperatures @ 20 mL/min

With regards to the already mentioned cooling line implemented in this third generation system, it was build out of a SS 316 tubbing of 1/16", wrapped around the reactor, allowing the minimum space possible between turns. The cooling liquid used was water, pumped at atmospheric pressure with the pump number 1 at maximum capacity (10 mL/min). Figure 2.34 also shows the beneficial effect that the cooling line had on decreasing the initial temperature of the reactor. In fact, a decrease of almost 30 DegC was obtained when cooling was performed in the experiment at 225 DegC. Furthermore, the cooling line has to be used only during thermal stabilization of the system, therefore, pumping of water must be stopped just before opening the valve V1.

2.3.1.3. Practical implications of the first liquefaction experiments

The initial liquefaction experiments were carried out in order to have an initial understanding of the liquefaction process and of the effect that the reaction time might have on it. At this stage of the project, it was assumed that no more modifications would be performed on the system, however, these experiments revealed many issues

that the system had, as well as they gave an insight of the enhancements needed to develop an optimal liquefaction system.

In order to keep an organize structure of this document, the results and description of these experiments will be given in the first section of the next chapter. By now, it is important to mention that after having performed some of the mentioned experiments (3 out of 8 runs), the back pressure regulator did not regulate the pressure anymore over 50 bar. To solve this issue, the BPR was unmounted and opened for inspection and cleaned. In fact, a large amount of organic and metallic little particles were found inside the BRP. The valve was cleaned and then reinstalled.

It was supposed that those metallic particles ended up inside the BPR as results of the large number of modifications that the system suffered, as long as every modification was a potential source of little particles getting into the tubbing. Regarding to the organic particles, it was noticed that the liquefaction stream leaving the cooling jacket had a temperature of nearly 135 DegC, temperature at which some liquefied products might still be reactive and very small in size, therefore, they might be able to pass thought the last filter, cooled in the BPR and then deposited in it. It was then decided to install a proper cooling that could pump water at lower temperatures and higher flow rates. A Cooling system Julao 250 was borrowed from SINTEF energy then connected to the cooling jacket. This system allowed to pump water at 5 DegC at a flow rate of 2 L/min. In fact, after having installed the pump, the temperature of the stream leaving the cooling jacket was reduced to 12 DegC and no more issues related to the BPR were observed. Figure 2.34 shows the particles deposited in the BPR as well as the ones collected in the first and second filter of the system.
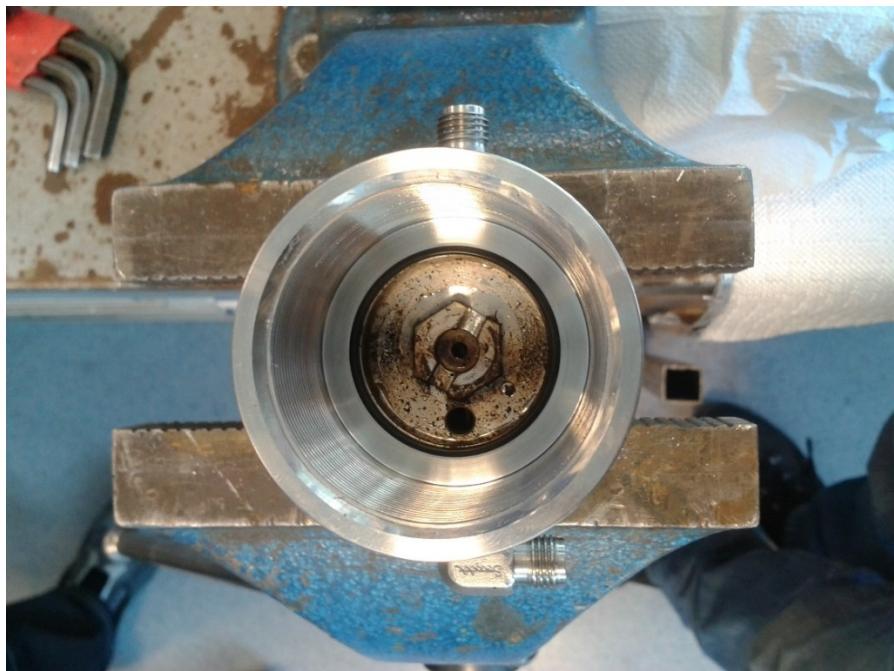
(a)

(b)

Figure 2.35. (a) Particles inside the BPR. (b) Particles collected from the first and second filter.

After having solved the issues with BPR, the experiments were continued and a new problem emerged in the run 6 out of 8. This time, a blockage in the heating coil was found. A cleaning process of the coil that involved flushing with pressurized air, then with pressurized water and finally, heat treatment at 780 DegC was performed. From

all the previous procedures some organic and metallic components were removed from the coil (identified by texture and smell). Unfortunately, it was verified that after the cleaning procedures, the coil was still blocked. To solve this problem, the coil was cut in 4 parts and then each part connected to the pump and water was flushed. By this methodology, the blocked coil was identified and replaced. It was then concluded that having the coil divided in four parts could be very convenient, especially when dealing with this kind of clogging problems.

As a parenthesis on this cleaning process, it was discovered that the most efficient technique to flush out possible particles deposited in the coil was:

- Connect the pump to the coil
- Leave the outlet of the coil to atmospheric pressure
- Start heating of the coil inside the furnace
- Flush the water

This technique has to be carefully carried out because evaporation and violent expulsion of the particles may occur. However, if after this cleaning process the coil is still blocked, it must be replaced. Figure 2.35 shows the particles extracted from the coil after having performed the mentioned steps.

Figure 2.36. Particles extracted from the heating coil

2.2.4. Fourth generation system.

Besides the addition of both the cooling system and the division of the heating coil in four parts, the fourth generation system involved also other enhancements as relocation of the pressurization lines, implementation of miniaturized inline filters, and finally the addition of a heating band around the dissolution reactor to improve its heating rate.

2.3.4.1. R&D Process

Relocation of the pressurization line was carried out having as justification the hypothesis that pressurizing the system in backwards direction might transport the particles trapped in the first and second filter upstream to the heating coil, where they deposit. Moving only the pressurization line to the inlet of the coil, but leaving the pressure measurement point just before the BPR gives to the system the guarantee of no backflows while keeping the ability of measuring the pressure in two different points of the system.

In the third generation system clogging problem were found not only in the heating coil, but also some blockage was present in the 1/16" line connecting the outlet of the heating coil with the dissolution reactor. In fact, this line had to be changed once for a complete new one. However, to improve the behaviour of the system against this type of inconvenient, a small piece of SS 316 cloth with pores of 1 um was placed inside the fitting connecting the heating coil and the dissolution reactor with this tubbing. It was noticeable the improvement that these to modification had over the system, as long as no further problems in this sense were observed in the system.

The addition of a heating band around the reactor was perhaps the most important enhancement of the fourth generation system. It allowed to add some valuable heat to the system that helped to further reduce the heating time of the dissolution reactor. At the beginning, the idea was to heat up the heating band to the reaction temperature as soon as the valve V1 was opened. However, major issues with this methodology were encountered given the poor control and heating time of the heating band itself. In fact,

with the controller available, stabilization of the heating band alone was nearly 10 minutes while the third generation system showed to have a shorter heating time of 5 minutes.

A second strategy used with the heating band was to apply some energy to the system but only for a short period of time, or in other words, to apply a step input signal of finite duration to the system. However, this technique was a very complicated solution taking into account that the amplitude of the step could not be controlled (clear disadvantage of using PWM for temperature control in AC systems), and that the duration of the impulse should be carefully calculated in order not to provide excessive energy to the system, then affecting the trend of the natural curve. Due to this inconvenient, many liquefaction experiments were ruined because a perfect heating up profile was not properly stablished. The effect that the temperature profile has one the liquefaction process is studied in detail in the next chapter.

After some trial and error experiments it was concluded that the best technique for properly using the heating band is:

- Turn on the cooling line of the reactor
- Turn on the heating up to a temperature of 40 Degrees
- Due to the thermal inertia of the system, the temperature will continue increasing until 45-50 DegC.
- As soon as the system reaches this temperature, cooling pumping must be shut down and valve V1 can be opened.

Following this steps, a faster and smoother temperature profile is obtained.

Finally, it was decided to re make the whole insulation of the system to improve the overall performance of the system, this factor might also have contributed to the nicer temperatures profiles obtained for this fourth generation system. Figures 2.37 to 2.39 shown in detailed the fully optimized liquefaction system.

Figure 2.37. Complete Liquefaction system.

Figure 2.38. Four Sections Heating Coil.

Figure 2.39. Dissolution Reactor and its cooling line in detail.

2.3.4.2. Performance Tests

The performance test carried out for the fourth generation system did not differ much from those made for the third generation system; in fact, it was observed that the behaviour of the furnace temperature vs dissolution reactor temperature curve did not vary much one from the other. This mean that the data obtained in the section 2.3.1.2 can be applied for the fourth generation system and that only little variations in the furnace temperature are needed in the moment of the experiment. Actually, such procedure was always followed in the experiments carried out in Chapter 3.

After having been working with the reactor for a while, it was noticed that an advantageous technique to even push further the already fast heating and stabilization times of the dissolution reactor was to set up the temperature of the furnace 6 DegC over the required one for the experiment. Such over temperature should then be compensated by injecting water in the cooling line of the reactor. After some empirical experimentation, it was found that water pumping at 0.35 mL/min should be started

6 DegC before the target dissolution temperature is reached. Moreover, such flow rate should be increase slowly up to 0.5 mL/min when the target temperature is reached. Since then, increments in the flow rate must be performed carefully, and according to the temperature increase in the reactor, up to 0.7-0.9 mL/min, flow rates at which the system stabilizes. This procedure has to be carefully carried out if one does not want to affect the temperature profile. For instance, it was discovered that even small variations of 0.1 mL/min can seriously affect the trend of the temperature, therefore disturbing heavily the dissolution rate of the biomass. This phenomena is later discussed in detail.

The results obtained from implementing this technique are shown in Figure 2.40.
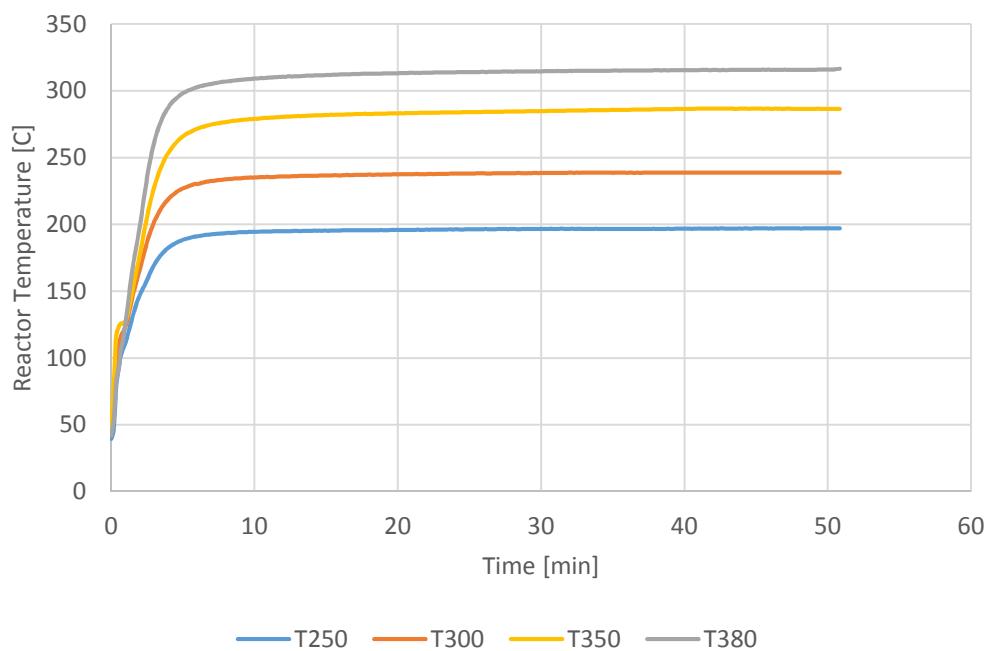
Figure 2.40. Heating time for different furnace temperature @ 20 mL/min

Chapter 3. Liquefaction Experiments

The effects that parameters such as residence time, reaction temperature and flow rate have on the dissolution of Norwegian Spruce are study in this section. Experiments showed that in sub-critical hydrothermal conditions dissolution of lignocellulose material can be as high as 95%.

3.1. Reaction time effects

3.1.1. Methodology

In order to have an initial insight of the process, two dissolution experiments were carried out at temperatures of 225 and 275 DegC, 100 Bar of pressure and flow rate of 20 mL/min.

The experiments were carried out for retention times of 15, 30, 45 and 60 mins. For each experiment, 1.5 grams of Norwegian Spruce Sawdust (dried overnight at 105 DegC) were loaded into the reactor and subjected to hydrothermal dissolution. After each experiment, the biomass residues in the system were recovered, dried overnight at the same temperature and further weighted. The total conversion efficiency was calculated for each experiment.

3.1.2. Results

The results obtained from this set of experiments, eight runs in total, are summarized in the Table 3.1.

T = 225 DegC					T = 275 DegC			
Time [min]	Initial mass [gm]	Final mass [gm]	Conversion Efficency [%]		Time [min]	Initial mass [gm]	Final mass [gm]	Conversion Efficency [%]
15	1.52	0.858	**43.55**		15	1.513	0.293	**80.63**
30	1.543	0.865	**43.94**		30	1.562	0.166	**89.37**
45	1.563	0.827	**46.09**		45	1.505	0.137	**90.90**
60	1.42	0.768	**46.1**		60	1.578	0.128	**91.89**

Table 3.1. Time effects in the conversion Efficiency.

According to the previous results, it seems that regardless the temperature, the dissolution process is mostly performed in the initial 15 minutes of reaction, and that temperature at which the process takes place greatly impacts its efficiency; in fact, for higher temperatures, higher conversion efficiencies are obtained.

While this experiments were carried out, it was noticed that the colour of the stream collected at the outlet of the system greatly change of colour with the passing time. Qualitatively speaking, it was noticed that at the beginning of the process, a liquid almost transparent was obtained. With the passing time, the collected liquid acquired a yellowish colour that increases in intensity with the passing time. At some point, after reaching a peak between the 5 and 10 minutes of reaction, the liquid started to lose its intense colour gradually until a point after 15 minutes, where it stabilized. It was also observed that for 225 DegC, the pale yellowish tone in the stream was never lost (even for reaction times of 60 mins), while for the experiment at 275 DegC, the stream reached a total transparent appearance after 30 minutes of reaction. Another difference between one and another experiment was the observed formation of foam, being this one much larger in the 225 DegC experiment. However, formation of foam always took place in the first minutes of the reaction, before the dissolution process reached its maximum peak. An example of the collected samples is given in the Figure 3.1.
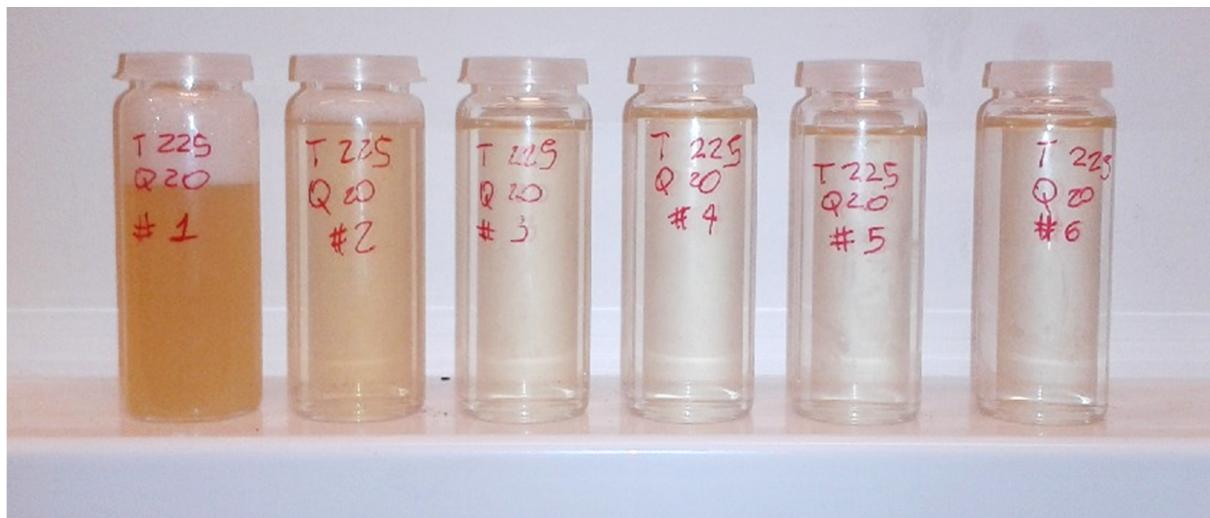
Figure 3.1. Collected Samples at 225 DegC, 20 mL/min at 15, 30, 45, 60, 75, 90 mins.

In addition to the observations of the liquid stream, it was also interesting to observe that the biomass recovered after the experiments also presented variations in colour according to the temperature and reaction time. For instance, at 225 DegC, the recovered spruce changed its appearance noticeable, acquiring a darker colour as the time of the reaction was increased. Figure 3.2, shows the chips recovered from the 225 DegC experiments after drying at atmospheric conditions for one day.

Figure 3.2. Recovered Spruce for the four different reaction times at 225 DegC. Top Right: 60 min. Top Left: 45 min. Bottom Left: 30 min. Bottom right: 15 min.

This results might suggest that once the liquefaction reactions are stopped at 15 mins, the spruce undergoes further torrefaction reactions that cause the darkening in the colour of the chips.

For the case of 275 DegC, differences in the colour of the chips recovered were not observed, but a very interesting fact is that despite these chips apparently occupied the same volume as the ones obtained at 225 DegC, their weigh was noticeable lower. Lastly, it is also important to mention that the color of the chips recovered from the experiment at 275 had a very dark color, very similar to the tone that charcoal has.

3.2. Reaction temperature effects

3.2.1. The initial experiences.

In order to properly stablish an adequate methodology for the study of the temperature effects, many experiments were carried out at different conditions of temperature, sampling time, drying method and equipment used for weighting the samples. In these initial experiences, the main problem encountered was in regards with the mass balances, as is described on next:

In a first set of experiments, the dissolution process was studied for samples of nearly 1.5 grams of spruce, water flow rate of 20 mL/min, 100 bars of pressure, and temperatures of 225 and 275 DegC. From each run, 10 samples of 7 mL each (20 seconds of collection) were collected every 100 seconds in small glass containers. After collection, 2 sub-samples of 1.5 mL each were subtracted from the original ones, and then poured into an Ependorf for further chemical analysis. The containers with the remaining liquid were put into an oven at 70 degC for drying until the point where all the water in the samples was evaporated. After evaporation (four days were required for total evaporation of water), the containers were weighted and a mass balance was performed.

The first mass balance came on with huge errors such as negative masses. The problems were attributed mainly to the fact that each container had been marked by first placing an adhesive tape on it, and then and identification code was written over. It could have happened that at 70 DegC, some of the components of the tape volatilized causing therefore a loss of mass. Also, it was noticed that after drying, some non-organic particles were trapped into the dried organic material. This suggested the need of covering the samples inside the oven, in order to avoid any particle going into the containers. Finally, it was also observed that the electronic weight meter was giving not accurate results, therefore, it was decided to use another balance.

In a second set of experiments at 225, 250 and 275 DegC, it was decided to increment both the volume of the collected sample up to 10 mL (30 seconds of collection), and the duration of the run up to 40 minutes. In addition, the sampling time (Time between collection of samples) in each run was varied as follows: 150 seconds for 225 DegC, 120 seconds for 250 DegC, and 90 seconds for 275 DegC. The containers were marked without any tape and a layer of aluminium foil was used to cover the samples inside the oven. In addition, it was decided to try higher drying temperatures such as 80 DegC for the samples of the 225 DegC experiment, 90 DegC for the ones of the experiment at 250 DegC, and 100 DegC for the samples obtained from the run carried out at 275 DegC; in order to reduce the long drying time that was causing a bottle neck in the schedule of the planned experiments. The results of the dried collected biomass from the dissolution process are plot in Figure 3.3, while the total conversion efficiency after 40 mins of reaction, calculated on the basis of (3), are given in Table 3.2.

Temperature [DegC]	Dissolution efficiency [%]
225	61.09
250	83.67
275	94.39

Table 3.2. Conversion Efficiency at different Reaction temperatures.
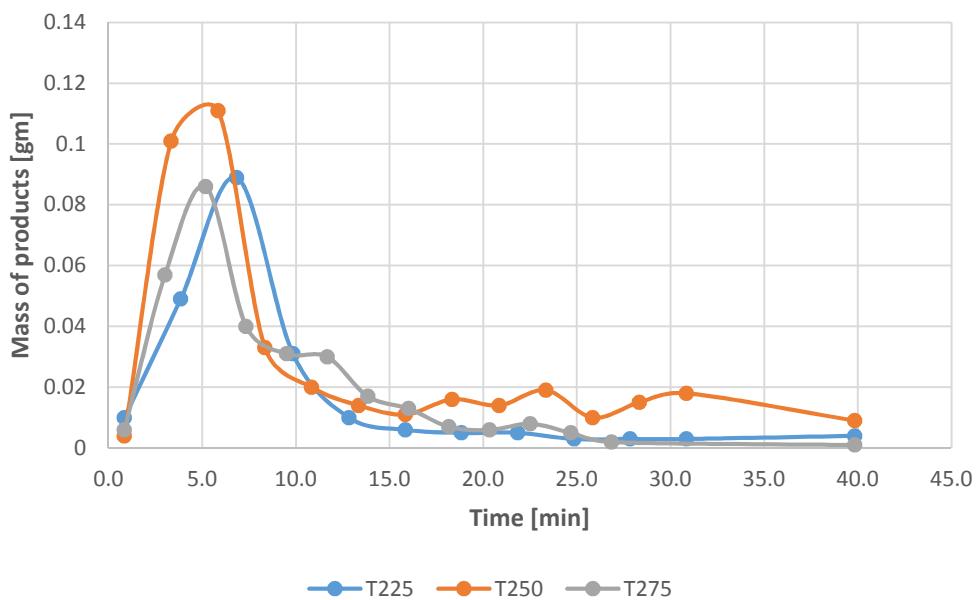
Figure 3.3. Mass of dried samples in time, for different reaction temperatures

The results in table 3.2, suggest that as the reaction temperature is increased, the dissolution efficiency also increases; whoever, the dynamic behaviour of the dissolution process shown in Figure 3.3, says that the conversion rate at 250 DegC is most of the time higher than that obtained at 275 DegC. However, this is not a coherent results because a sustained higher conversion rates at 250 DegC will lead to higher yield of total dissolved mass than that obtained at 275 DegC.

The disagreement between these two results might be caused for two reasons: firstly, the use of different sampling times might have caused disagreement between the material collected at a given time, and secondly, the high temperature used for drying the 275 DegC samples, (100 DegC), might have caused evaporation of important compounds in the samples. Despite the problems in the mass balances (especially for the experiment at 275 DegC), it could be concluded that a samples of 10 mL were large enough to properly perform the mass balances required; however, for these last experiments, it is deducted that the maximum drying temperature must not exceed the 80 DegC.

3.2.2. Methodology

The optimized methodology for carrying out the study of the temperature effects is described as follows:

- The initial mass loaded into the reactor was increased up to 2.4 grams. (Maximum capacity of the reactor)
- The analysis of the Temperature effect was carried out for five different Temperatures: 200, 225, 250, 275 and 300 DegC.
- Each collected sample had 10 mL of products.
- The Sampling Time for all cases was 45 seconds for the initial 15 minutes, afterwards, it was doubled every two samples until a the experiment reached a time of 40 minutes.
- From each experiment, 20 Samples were taken.
- All experiments were carried out at 100 BAR
- The collected samples of all the experiments were put in a cardboard rack and dried for 5 Days in a big furnace at 80 DegC. Figure 3.5 shows the rack of samples. Figure 3.4 shows the first 10 collected samples for the 225 and 275 experiments.
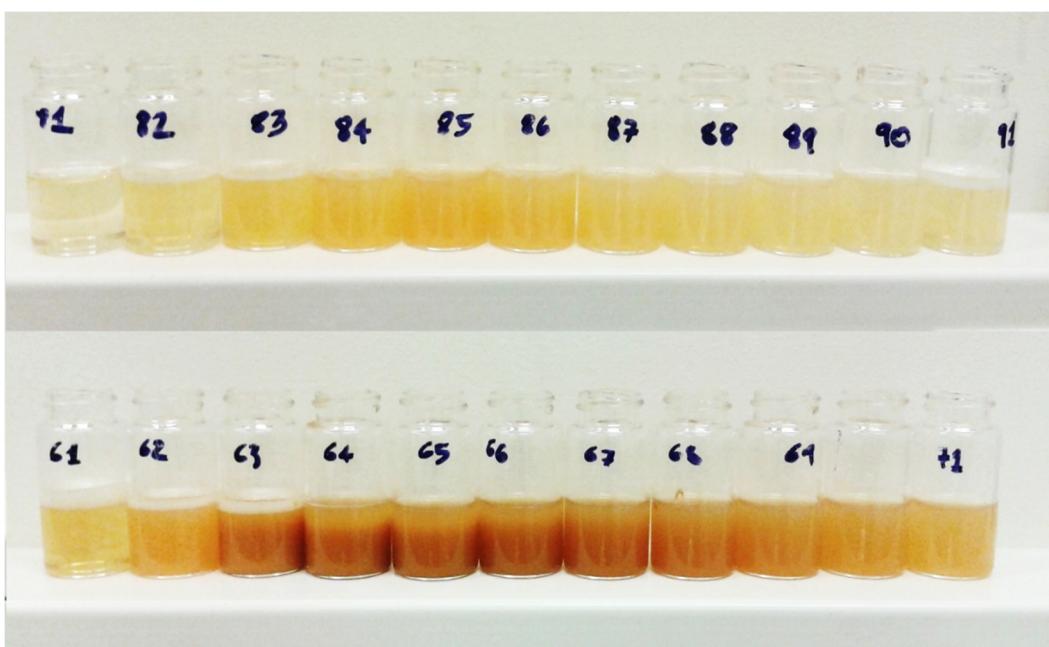
Figure 3.4. UP: collected samples for the 225 DegC. Down: collected samples for the 275 DegC.

Figure 3.5. Rack of Collected samples to be dried.

The experiments carried out according to the previous methodology did not provide immediate satisfactory results, mainly due to the fact that in some experiments leaks affected the temperature profile in the reactor, therefore damaging the normal behaviour of the system. This issues forced, in some cases, to repeat the experiments up to 3 times, until a nice profile was obtained.

3.2.3. Results

3.2.3.1. Conversion Efficiency

The conversion efficiency was calculated according to the technique described in the section 2.3.1.2, and the results are summarized in Figure 3.6. This conversion efficiency accounts for the total dissolved biomass after 40 mins of reaction.
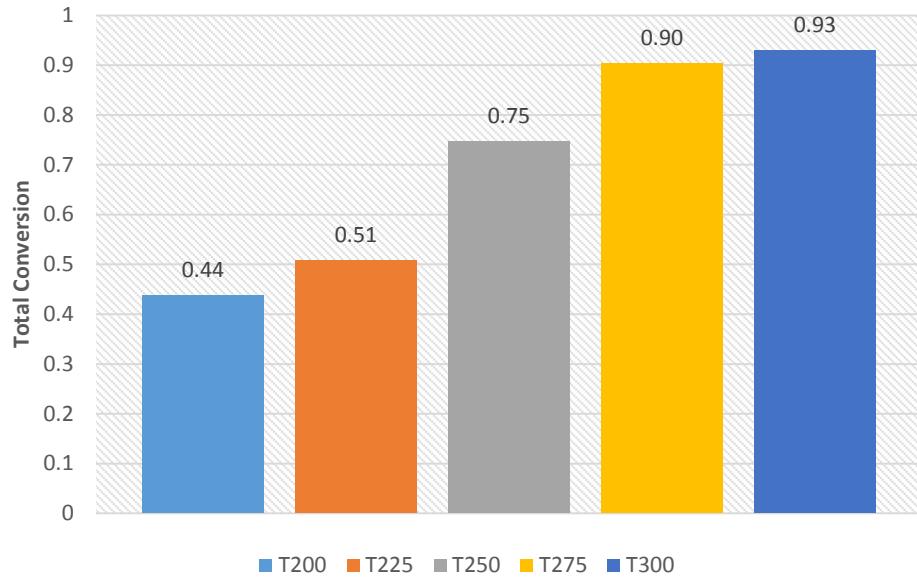
Figure 3.6. Conversion Efficiency of the dissolution process for different Temperatures.

On the contrary to the results obtained by Hashaikeh [30], we observe that the dissolution efficiency is highly dependent on temperature, and that yields of dissolved products increase as the reaction temperature does.

The results also show a rational trend in accordance with composition of the Spruce. In fact, at 200 and 225 DegC, only dissolution of the lignin and hemicellulose part of the spruce was expected. Having into account that these two components account for up to 55% of the total mass of the spruce, the obtained conversion efficiencies not higher than 51% for both experiments match perfectly the theoretical dissolution temperatures with our results. Based on the previous observation, one can conclude that after HTT at 225 DegC, only the cellulose part remains in the spruce.

An interesting observation can be given from the experiment at 250 DegC, temperature for which dissolution of cellulose was not expected. However, the reached conversion efficiency of 75% suggests that at this temperature a phenomena in which total dissolution of hemicellulose and lignin, as well as a partial dissolution of non-crystalline cellulose occurred. A similar results were reported previously in [30].

3.2.3.2. Dynamic behaviour

The dynamic behaviour of the dissolution process is studied by means of plotting the mass collected in each container, for each experiment vs time. The results are summarized in Figure 3.7.
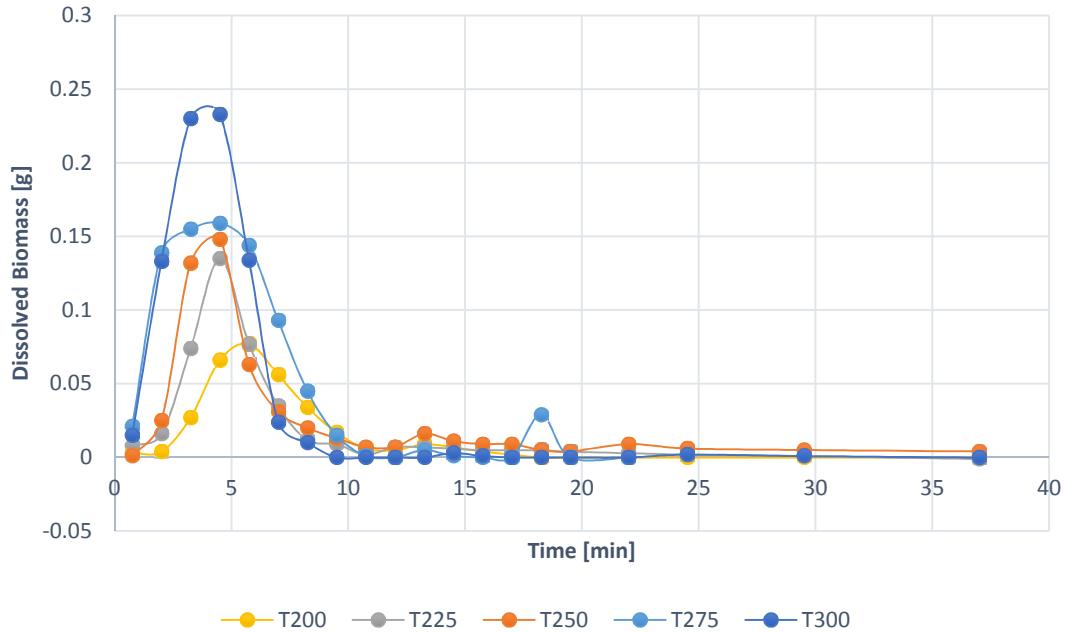
Figure 3.7. Dynamic behaviour of the dissolution process for different temperatures.

The study of the dynamic behaviour of the dissolution mechanism reveals that both the amount of mass dissolved in time, and the time required for completing the dissolution process are highly dependent on temperature. It is also noticed that the dissolution profile has a bell shape for all the cases. The results obtained in this study are coherent with those obtained in [30] with regards to the shape of this curve, as reported in Figure 3.8. However, in this study was found for all cases that as the temperature increased, the instantaneous dissolved mass also increased until the point where its maximum was reached. Another similarity of both studies is the tendency of the peak of moving to the left as the temperature increased. The movement of this peak can be interpreted as an acceleration of the process, therefore reducing its total reaction time.
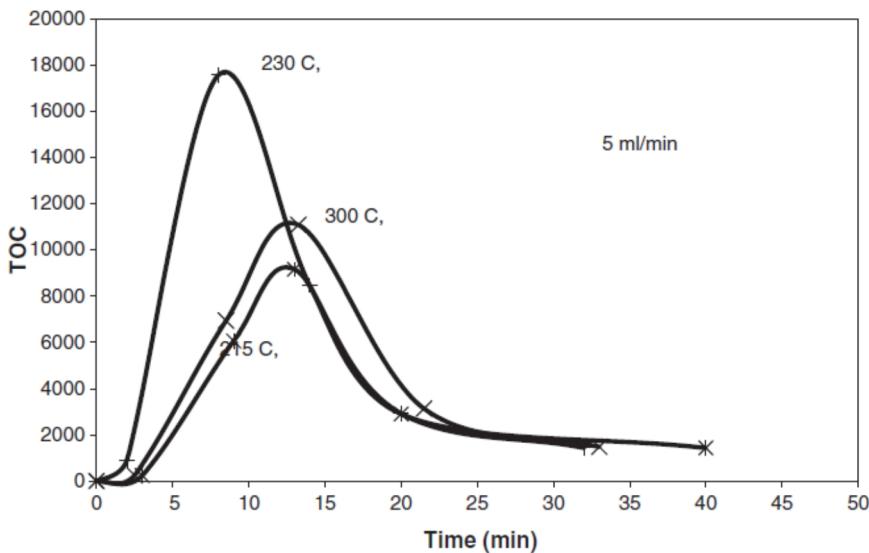
Figure 3.8. Dynamic behaviour of the dissolution process for different temperatures reported by [30].

It is also interesting to see that at medium temperatures of 225, 250 and 275 DegC, all the peaks reached values of nearly 0.15 grams for the instantaneous dissolved biomass. In the other hand, for 200 and 300 DegC, the peaks were 0.01 and 0.24 respectively. These results show some patterns in the dissolution process that one can associate with the reaction of certain specific biomaterials. For instance, for 200 DegC, the low peak suggests that only hemicellulose has been dissolved. For the medium peaks, dissolution of only hemicellulose and lignin is expected. Finally for 300 DegC, Dissolution of all the three components, cellulose, hemicellulose and lignin is expected to occur.

In addition to the previously mentioned dissolution stages, based on temperature, it is important to keep in mind that also time plays a very important role in this process. If, for instance, the curve at 275 DegC is studied carefully, it is possible to notice that despite the fact that its peak apparently reached a value where only dissolution of hemicellulose and lining is expected, its slow decay after the peak (if compared with the 300 Deg curve) suggests that most of the cellulose dissolution occurs after the peak. In fact, a very similar behaviour is observed for the curve at 200 DegC, when it is compared with the 225 and 250 DegC ones. For the former temperature, it would be possible to conclude that hemicellulose dissolution occurs mostly in the first part of the reaction (from zero to the peak), while lignin dissolution occurs in the second one (from the peak until minute 10).

On the contrary to what have been mentioned for the particular behaviour of the curves at 200 DegC and 275 DegC, the curve at 250 DegC shows a very fast dissolution behaviour after and before the peak. In fact, it is possible to say that at this temperature, the reaction happens as fast as the one at 300 DegC, but with very little dissolution of cellulose.

In order to have a more precise understanding about the influence that temperature and reaction time have on the process, the cumulative normalized mass (NAUC) is plotted in Figure 3.9. The cumulative data is calculated by making an approximation of the area under the curve (AUC) by the trapezoidal method according to:

$$AUC = \frac{b-a}{2*n} * \sum_{k=1}^{n} y_k \qquad (5)$$
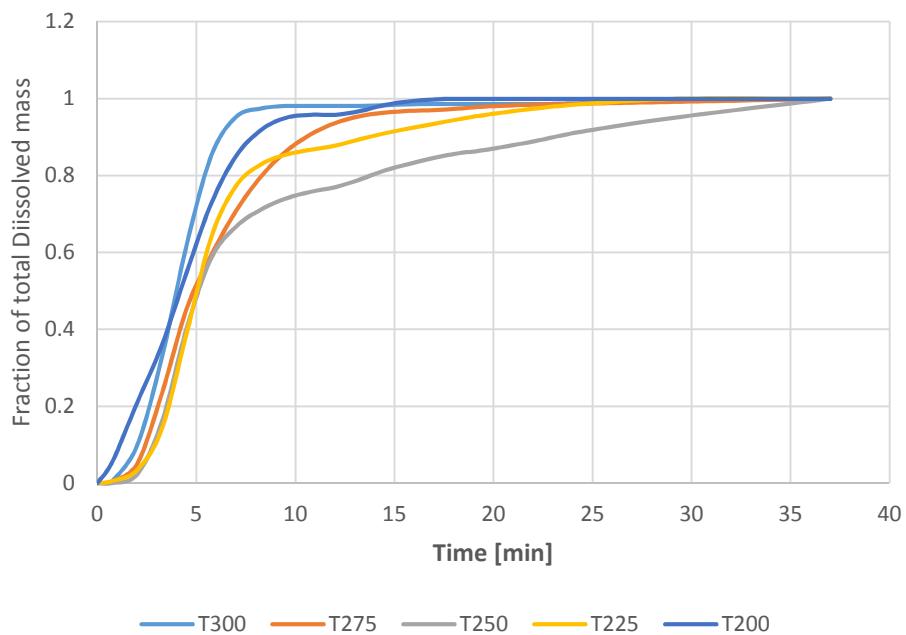
Figure 3.9. Normalized Accumulative dissolved mass.

It is very interesting to note that for most of the temperatures, except 250 DegC, the conversion of biomass is a very fast process that reaches 80% of the total dissolved mass in the first 10 mins. It is also noticeable that when the instantaneous peak of

dissolution occurs, a dissolution of at least 50% has been already reached in all the cases. The trends in the accumulative normalized dissolved mass support the previous observation about what type of biomass component is dissolved at a certain temperature and at a certain moment. For instance, for 300 DegC, a very fast dissolution of all components is observed. For 275, dissolution of all components is also observed, but the time required is almost twice as the one at 300 DegC. At 250, it is very interesting to see that reaction takes a very long time. In fact, it can be deducted that most of the dissolution of hemicellulose and lignin occurred in the first 7 minutes of reaction, but since then on, a very slow dissolution process of cellulose takes place. For 225 DegC, it can be seen that a fast dissolution of hemicellulose is obtain in the first 10 minutes, and that since then a slow dissolution of lignin is carried out. Finally, for 200 DegC, A fast dissolution of hemicellulose and a little one of lignin are observed.

3.2.3.3. Mass Balances

Figure 3.10 shows the results of the mass balances calculated for each temperature, for a time reaction of 40 minutes, according to the formulas:

$$x_{SR} = \frac{Solid\ Residues\ [g]}{Initial\ Biomass\ [g]} * 100\% \qquad (6)$$

$$x_{WSP} = \frac{Area\ under\ the\ curve\ [g]}{Initial\ Biomass\ [g]} * 100\% \qquad (7)$$

$$x_{Lost} = (1 - x_{SR} - x_{WSP}) * 100\% \qquad (8)$$
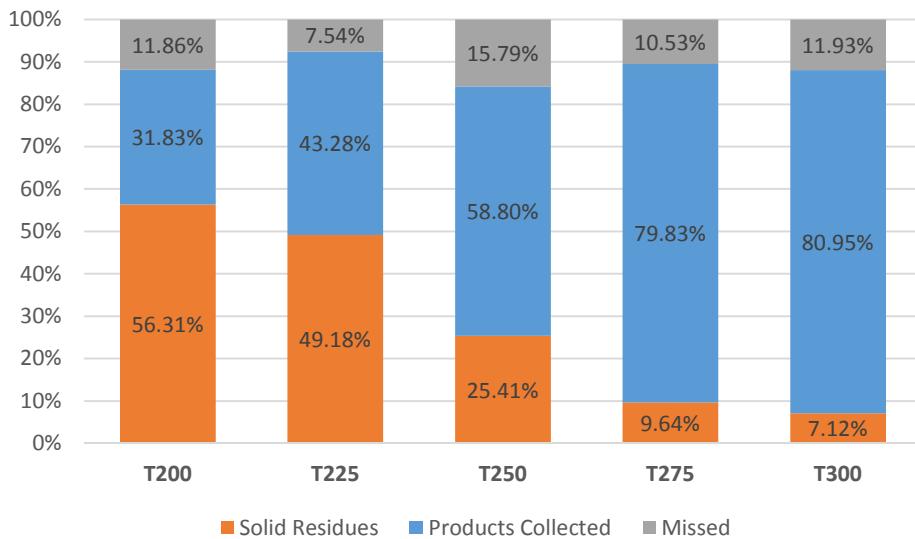
Figure 3.10. Mass Balances of the experiments.

It has to be said that Figure 3.10 is a more detailed graph than Figure 3.6, where only the conversion of the biomass is accounted for. In fact, it has to be noticed that when the corresponding fractions to products collected and mass misses are added, they are equal to the total fraction of mass converted. One interesting observation regarding this experiment is that the fraction of mass lost in all experiments has more or less the same value, except for the experiment at 250 DegC. One then might conclude that such mass fraction is inherent to the process itself, instead of being related to any conversion of biomass to gas. In fact, the complex structure of the system can favour the accumulation of particles in the valves, filters and in the BPR. These particles are indeed are very difficult to be recovered.

The mass balances also reveal the coherence that exists between theory and the obtained results. Higher temperatures lead to more Water soluble products and less solid residues.

It is also very important to remark that even at the high temperature of 300 DegC, all the liquefied products maintained their water soluble nature. In order to confirm this hypothesis, 3 mL of dichloromethane, and 3 mL of Hexane were added to one of the samples of the experiment at 300 DegC. As expected the DCM went to the bottom of the container while the hexane stayed on the top. After 12 hours, it was observed that the colour of the two non-polar phases did not change and they maintained their

transparent nature. Under this observation, it can be concluded that no oily phase was obtained from the dissolution experiments here carried out. Figure 3.11 shows the three phase sample.

Figure 3.11. Sample collected from an experiment at 300 DegC + DCM + Hexane

Chapter 4. General Conclusions

In order to properly study the effect that temperature has on the hydrothermal liquefaction of biomass, a semicontinuous fixed bed reaction system was design, developed, tested and used. The system built was based on a Parr Continuous reaction system able to work at high temperature, and it was proved to have good performance for hydrothermal liquefaction processes at conditions up to 300 DegC and 100 Bar.

Woody biomass is found to be a very attractive raw material for the production of chemicals and biofuels. The number of basic chemicals that can be obtained via hydrothermal treatment of biomass without the use of any other chemical is vast.

Despite the fact that the system is able to reach higher temperatures, higher pressures are not recommended due to the fact that little leakages are present in the valves. The issue of these leakages can be solved only if a double system of valves back to back is implemented. However, using a double valve system will increase the number of valves in the system from 3 to 5, with an increase in the probability of losing more mass is by its deposition in the new added elements.

The system could be enhanced with a larger reactor, as the one that was also built in the framework of this Thesis, however, an additional heating band with a proper controller is required. It has been proven that the direct heating of the reactor via the hot compressed water itself is effective only for small reactors, with a capacitiy not larger to 5 mL.

The study of the original Parr system revealed the numerous heat transfer problems present in the furnace-reactor arrangement. In fact, it can be concluded that only a very short length of the original reactor offers a stable and isothermal temperature profile for only very low flow rates of water. However, in order to improve the heat transfer inside the furnace, it is proposed to fill up the gap of air with any conductive material able to withstand temperatures of up to 400 DegC. Some examples of materials could be table salt or cooper powder, however, it is necessary to keep in mind the flammability nature of this last material.

It is also advisable to replace the fixed bed reactor after 10 runs, as long as the wear created from the opening and closing of the reactor is unavoidable. Overuse of the reactor lead to leakages that affect the temperature profile of the system, therefore affecting the liquefaction process itself, as well as increasing safety risks.

It can be said also that the original Parr reactor system can be used for liquefaction experiments if a slurry pump is added to the system, and if pumping of the biomaterial is performed at very low flow rates. However, works to improve the heat transfer phenomena in the furnace-reactor arrangement have to be done.

The use of an appropriate scale, as well as the use of glove is a must when weighting the collected samples, in fact, it is advisable not to use the electronic balance in the chemistry room of the thermal lab, but instead, to use the one in the TGA room.

After experiments, it is always recommended to flush the system with water at very high flow rates, and to clean the BPR once problems in regulation in the pressure are noticed.

With regards to the dissolution experiments, it can be said that in order to obtain bio oil from the dissolved material, further treatments are absolutely required. An interesting option of further upgrading of the collected products is the addition of one block able to perform Adol Condensation reactions that can transform many of the WSP as the 5-HMF into chains of hydrocarbons of c-20 length.

It was found that the developed system offers a very fast heating rate that allows for the study of biomass dissolution at very short reaction times. The system helped to obtain a set of data that cannot be derived either from batch and continuous reactors. From the experiments, it was observed that at suitable temperatures, reaction times can be as low as 5 minutes, while for non-optimal temperature conditions, the dissolution reactions can take up to 40 minutes.

The dissolution process was found to be greatly affected by temperature and by the heating rate of the system. The experiments revealed that a maximum dissolution of

biomass can be obtained fast at 300 DegC, without any intermediate. In fact, it can be concluded that a two steps dissolution as was proposed by [30], is not required.

It can be also concluded that the dissolution process can be designed to have a very high selectivity of the products obtained, just by adjusting the reaction temperature. In fact, it is hypothesised that this process could be very effectively implemented inside the context of the novel concepts of bio refinery.

Having into account that the process here designed proved to have very good dissolution efficiencies and selectivity, a major issue to improve it is the amount of water required for the process. In fact, one can conclude that for dissolving 90% of an initial charge of 2.4 grams of biomass, a total amount of 140 mL of water is required at 300 DegC and 100 Bar. Reduction in water consumption will lead to a more efficient process, not only because less energy would be invested in the heating and pumping process, but also because it will facilitate the recovery of the highly diluted compounds in the resulting stream.

References

1. UN Report; Sustainable Bioenergy: A Framework for Decision Makers; April 2007

2. Review of EU Biofuels Directive; Public consultation exercise; April- July 2006

3. Chisti Y; Biodiesel from Microalgae; Biotechnology Advances 25 (2007) 294–306

4. Andrew A. Peterson, Fre´de´ric Vogel, Russell P. Lachance, Morgan Fro¨ling, Michael J. Antal, Jr, Thermochemical biofuel production in hydrothermal media: A review of sub- and supercritical water technologies, The Royal Society of Chemistry 2008.

5. R. Lachance, unpublished data, 2007.

6. Z. Srokol, A. G. Bouche, A. van Estrik, R. C. J. Strik, T. Maschmeyer and J. A. Peters, Hydrothermal upgrading of biomass to biofuel; studies on some monosaccharide model compounds, Carbohydr. Res., 2004, 339(10), 1717–1726.

7. G. Bonn and O. Bobleter, Determination of the hydrothermal degradation products of D-(U-14C) glucose and D-(U-14C) fructose by TLC, J. Radioanal. Nucl. Chem., 1983, 79(2), 171–177.

8. Mitsuru Sasaki, Bernard Kabyemela, Roberto Malaluan, Satoshi Hirose, Naoko Takeda, Tadafumi Adschiri, Kunio Arai, Cellulose hydrolysis in subcritical and supercritical water, Journal of Supercritical Fluids 13 (1998) 261–268.

9. Yan Zhao,Wen-Jing Lu, Hong-TaoWang, Supercritical hydrolysis of cellulose for oligosaccharide production in combined technology, Chemical Engineering Journal 150 (2009) 411–417.

10. X.J. Ma, S.L. Cao, L. Lin, X.L. Luo, H.C. Hu, L.H. Chen, L.L. Huang, Hydrothermal pretreatment of bamboo and cellulose degradation, Bioresource Technology 148 (2013) 408–413.

11. Y. Roman-Leshkov, C. J. Barrett, Z. Y. Liu and J. A. Dumesic, Production of dimethylfuran for iquid fuels from biomass-derived carbohydrates, Nature, 2007, 447(7147), 982–985.

12. D. A. Nelson, P. M. Molton, J. A. Russell and R. T. Hallen, Application of direct thermal liquefaction for the conversion of cellulosic biomass, Ind. Eng. Chem. Prod. Res. Dev., 1984, 23(3), 471–475.

13. Danilo A. Cantero, M. Dolores Bermejoa, M. José Cocero, Kinetic analysis of cellulose depolymerization reactions in near critical water, J. of Supercritical Fluids 75 (2013) 48– 57.

14. W. Schwald and O. Bobleter, Hydrothermolysis of cellulose under static and dynamic conditions at high temperatures, J. Carbohydr. Chem., 1989, 8(4), 565–578.

15. T. Adschiri, S. Hirose, R. Malaluan and K. Arai, Noncatalytic conversion of cellulose in supercritical and subcritical water, J. Chem. Eng. Jpn., 1993, 26(6), 676–680.

16. K. Mochidzuki, A. Sakoda and M. Suzuki, Measurement of the hydrothermal reaction rate of cellulose using novel liquid-phase thermogravimetry, Thermochim. Acta, 2000, 348(1–2), 69–76.

17. M. Sasaki, Z. Fang, Y. Fukushima, T. Adschiri and K. Arai, Dissolution and hydrolysis of cellulose in subcritical and supercritical water, Ind. Eng. Chem. Res., 2000, 39(8), 2883–2890.

18. M. Sasaki, T. Adschiri and K. Arai, Kinetics of cellulose conversion at 25 MPa in sub- and supercritical water, AIChE J., 2004, 50(1), 192–202.

19. O. Bobleter, Hydrothermal degradation of polymers derived from plants, Prog. Polym. Sci., 1994, 19, 797–841.

20. G. Garrote, H. DomõÂnguez, J. C. Parajo, Hydrothermal processing of lignocellulosic materials, Holz als Roh- und Werkstoff 57 (1999) 191±202 Ó Springer-Verlag 1999.

21. Xuejun Liu∗, Meizhen Lu, Ning Ai, Fengwen Yu, Jianbing Ji, Kinetic model analysis of dilute sulfuric acid-catalyzed hemicellulose hydrolysis in sweet sorghum bagasse for xylose production, Industrial Crops and Products 38 (2012) 81– 86.

22. D. Edwin, L. J. J. Laarhoven, I. W. C. E. Arends, P. Mulder, J. Anal. Appl. Pyrolysis 2000, 54, 153.

23. Shimin Kang, Xianglan Li, Juan Fan, Jie Chang, Hydrothermal conversion of lignin: A review, Renewable and Sustainable Energy Reviews 27 (2013) 546–558.

24. Wahyudiono, Takayuki Kanetake, Mitsuru Sasaki, Motonobu Goto, Decomposition of a Lignin Model Compound under Hydrothermal Conditions. Chem. Eng. Technol. 2007, 30, No. 8, 1113–1122.

25. KangS, LiX, FanJ, ChangJ. Classified separation of lignin hydrothermal liquefied Products. Industrial & Engineering Chemistry Research 2011; 50:11288–96.

26. BarbierJ, Charon N, Dupassieux N, Loppinet-Serani A, Mahe L, Ponthus J, etal. Hydrothermal conversion of lignin compounds. A detailed study of fragmentation and condensation reaction pathways. Biomass Bioenergy 2012; 46:479–91.

27. http://www.parrinst.com/products/specialty-custom-systems/5400-continuous-flow-tubular-reactors/applications-2/

28. M. Mosteiro-Romero, F.Vogel, A.Wokaun, Liquefaction of wood in hot compressed water. Part1 — Experimental results, Chemical Engineering Science 109(2014)111–122.

29. Incropera, Dewitt, Bergman, Lavine, Fundamentals of Heat and Mass transfer, Sixth edition, John Willey & Sons, 2007.

30. R. Hashaikeh, Z. Fang, I.S. Butler, J. Hawari, J.A. Kozinski, Hydrothermal dissolution of willow in hot compressed water as a model for biomass conversion, Fuel 86 (2007) 1614−1622.

31. Xin Lu, ShiroSaka, Hydrolysis of Japanese beech by batch and semi-flow water under subcritical temperatures and pressures, Biomass and bioenergy 34(2010)1089−1097.

32. Yukihiko Matsumura, Tomoaki Minowa, Biljana Potic, Pascha R.A. Kersten, Wolter Prins, Willibrordus P.M. van Swaaij, Bert van de Beld, Douglas C. Elliott, Gary G. Neuenschwander, Andrea Kruse, Michael Jerry Antal Jr., Review: Biomass gasification in near- and super-critical water: Status and prospects, Biomass and Bioenergy 29 (2005) 269−292.

33. Frederique Bertaud, Bjarne Holmbom, Chemical composition of earlywood and latewood in Norway spruce heartwood, sapwood and transition zone Wood. Wood Sci Technol (2004) 38: 245−256